

We appreciate the editor and both referees for their valuable and insightful comments, which have greatly improved our manuscript. Below we describe the modifications made according to their comments. For clarity, comments are given in *italics* and blue, and our responses are given in plain text. The line numbers within brackets indicate the location of the modifications in the revised manuscript. The revised manuscript with all revisions tracked is appended at the end of this document.

## -Referee#1-

*There are many researches focusing on reasons, causes and modelling of nonstationarity of hydrological extremes such as: Xihui Gu, Qiang Zhang, Vijay P. Singh, Peijun Shi, 2017. Nonstationarities in the occurrence rate of heavy precipitation across China and its relationship to climate teleconnection patterns. International Journal of Climatology, DOI: 10.1002/joc.5058. Xihui Gu, Qiang Zhang, Vijay P. Singh, Peijun Shi, 2017. Changes in magnitude, frequency and timing of heavy precipitation across China and its potential links to summer temperature. Journal of Hydrology, 547, 718-731. Xihui Gu, Qiang Zhang, Vijay P. Singh, Peijun Shi, 2017. Nonstationarity in timing of extreme precipitation across China and impact of tropical cyclones. Global and Planetary Change, 149, 153-165. Xihui Gu, Qiang Zhang, Vijay P. Singh, Lin Liu, 2016. Nonstationarity in the occurrence rate of floods in the Tarim River basin, China, and related impacts of climate indices. Global and Planetary Change, 142, 1-13. Qiang Zhang, Xihui Gu, Vijay P. Singh, Mingzhong Xiao, Xiaohong Chen, 2015. Evaluation of flood frequency under non-stationarity resulting from climate change and human activities in the East River basin, China. Journal of Hydrology, 527, 565-575. Qiang Zhang, Xihui Gu, Vijay P. Singh, Mingzhong Xiao, Chong-Yu Xu, 2014. Stationarity of annual flood peaks during 1951-2010 in the Pearl River basin, China. Journal of Hydrology, 519, 3263-3274. What are the motivations, research objectives and novel points of this current study when compared to standing researches? My strong suggestion is that thorough literature review is pretty necessary. New findings, new ideas, new methods, if any, should be pointed out with enough citations to justify authors' statements.*

**AUTHORS' REONSE:** Thank you for introducing the overlooked references and for the good suggestion of enhancing the literature review. Following the advice of the reviewer, we have made a more comprehensive literature survey by citing and discussing important recent publications in the field, including those introduced by the reviewer. We have also improved the description of motivations, research objectives and novel points of this current study. The related paragraphs have been changed into the following:

“In hydrological analysis and design, conventional frequency analysis estimates the statistics of a hydrological time series based on recorded data with the stationary hypothesis which means that this series is ‘free of trends, shifts, or periodicity (cyclicity)’ (Salas, 1993). However, global warming and human forces have changed

climate and catchment conditions in some regions. Time-varying climate and catchment conditions can affect all aspects of the flow regime, i.e. changing the frequency and magnitude of floods, altering flow seasonality, and modifying the characteristics of low flows, etc. The hypothesis of stationarity has been suspected (Milly et al., 2008). If this problematic method is still used, the frequency analysis may lead to high estimation error in hydrological design. Therefore, considerable literatures have introduced the concept of hydrologic nonstationarity into analysis of various hydrological variables, such as annual runoff (Arora, 2002; Jiang et al., 2017; Jiang et al., 2015; Liu et al., 2017; Xiong et al., 2014; Yang and Yang, 2013), flood (Chen et al., 2013; Gilroy and Mccuen, 2012; **Gu et al., 2016**; Kwon et al., 2008; López and Francés, 2013; Tang et al., 2015; Xiong et al., 2015b; Yan et al., 2016; **Zhang et al., 2014**; **Zhang et al., 2015**), low flow (Du et al., 2015; Jiang et al., 2014; Liu et al., 2015), precipitation (Cheng and AghaKouchak, 2014; **Gu et al., 2017a, b, c**; Mondal and Mujumdar, 2015; Shahabul Alam et al., 2014; Villarini et al., 2010) and so on. Compared with the literatures on annual runoff, floods and precipitation, the literatures on the nonstationary analysis of low flow are relatively limited.” [Lines 62-78]

“To our knowledge, compared with the nonstationary flood frequency analysis, the studies on the nonstationary frequency analysis of low-flow series is not very extensive because of incomplete knowledge of low flow generation (Smakhtin, 2001). Most of these studies explain nonstationarity of low-flow series only by using climatic indicators or a single indicator of human activity. However, the indicators of catchment conditions (e.g. recession rate) related to physical hydrological processes have seldom been attached in nonstationary modeling of low flow series. This lack of linking with hydrological process makes it impossible to accurately quantify the contributions of influencing factors for the nonstationarity of low flow series, and such a scientific demand for tracing the sources of nonstationarity of low-flow series and qualifying their contributions motivated the present study...” [Lines 100-109]

“The goal of this study is to trace origins of nonstationarity in low flows through developing a nonstationary low-flow frequency analysis framework with the consideration of the time-varying climate and catchment conditions (TCCCs) and human activity (HA). In this framework, the climate and catchment conditions are quantified using the eight indices, i.e., meteorological variables (total precipitation  $P$ , mean frequency of precipitation events  $\lambda$ , temperature  $T$  and potential evapotranspiration  $ET$ ), basin storage characteristics (base-flow index  $BFI$ , recession constant  $K$ ) and aridity indexes (climate aridity index  $AI_{ET}$ , the recession-related aridity index  $AI_K$ ). The specific objectives of this study are: (1) to find the most important index to explain the nonstationarity of low-flow series; (2) to determine the best subset of TCCCs indices and/or human activity indices (i.e., population  $POP$ , irrigation area  $IAR$ , and gross domestic product  $GDP$ ) for final model through stepwise selection method to identify nonstationary mode of low-flow series; and (3) to quantify the contribution of selected explanatory variables to the nonstationarity.” [Lines 131-142]

*There are no exact and/or results included in the Abstract section. Or only limited words describing results. More details and particularly in a quantitative way should be provided for description of results and conclusions*

**AUTHORS' REONSE:** The reviewer is correct. In the modified abstract, we have provided more quantitative results and conclusions. In the revision of the second part of the Abstract, the description of results and findings has been modified as following:

“The results from stepwise regression for the optimal explanatory variables show that the variables related to irrigation, recession, temperature and precipitation play an important role in modeling. Specifically, analysis of annual minimum 30-day flow in Huaxian shows that  $AI_K$  is of the highest relative importance among the optimal variables, followed by *IAR* (note to reviewer: *Irrigated area – a newly added index in the revised version*), *BFI* and  $AI_{ET}$ ; and nonstationary GA distribution model with these optimal variables has an AIC value of 207.0, while the AIC values of other models just with  $AI_K$  or time as explanatory variables or without any variable are 217.4, 225.5, 232.3, respectively. We conclude that the incorporation of multiple indices related to low-flow generation permits tracing various driving forces.” [Lines 29-36]

*In Introduction section, it was noticed that there are numerous researches focused on nonstationary low flow frequency analysis. However, no novel points were listed and hence research motivations were not well justified. Besides, as a tributary of the Yellow River, evaporation or evapotranspiration, irrigation, population, GDP and so on should be included as factors influencing low flow changes. Related works have been done using Budyko framework by Prof. Dawen Yang from Tsinghua University and Prof. Qiang Zhang from Beijing Normal University and other colleagues from China. Besides, I still have no idea about how the authors developed the framework to evaluate low flow frequency from a nonstationary perspective.*

**AUTHORS' REONSE:** Thanks to the reviewer for pointing out this. Firstly, in the introduction section, the related part has been reorganized and modified in order to clarify our research motivations more clearly. Related part for study motivation, refer to the response of the first comment above.

Secondly, following the reviewer's advice, besides the following indices ( $K$ ,  $AI_K$  and *BFI*) that are related to human activities and the indices ( $K$ ,  $AI_K$  and *BFI*) that are linked to physical hydrological processes, in the revised version, we have included the irrigation area (*IAR*), the Gross Domestic Product (*GDP*), and population (*POP*) indices. The process of their change with time has been presented (see Fig. 5 in the revised manuscript). The Pearson correlation coefficients between low-flow series and these indices have been presented (see Fig. 6 in the revised manuscript). The models (M2b, M5, and M6, as described in Table 2 in the revised manuscript) are added. The summary of their results have been presented in Table 5 in the revised manuscript. Analysis of all new results has been shown in Figs. 7, 8, 9, 10 and 11 in the revised manuscript. Besides, we have added the following statements in the discussion section

in the revised manuscript.

“The related researches (Jiang et al., 2015; Yang and Yang, 2011; Yang and Yang, 2013; Zhang et al., 2015) have applied the Budyko framework to analyze the impacts of climate change and/or human activity on annual runoff. Indeed, for annual runoff, the Budyko framework is a good method because it used the mean annual water-energy balance equation to consider generation process of total runoff. Unfortunately, to our knowledge, there is a lack of equation derived from basic physics laws for generation process of low flows. Therefore, we emphasize the importance of TCCCs variables to modeling of low-flow nonstationarity.” [Lines 507-513]

Thirdly, the framework is composed of the time varying and GLM methods, and the method of stepwise selection for TCCCs indices and human activity indices. And to address this comment, we have added a flow chat of methodology (Fig. 1 in the revised manuscript) to explain how the framework is organized.

*In Method section, a working framework should be formulated besides some descriptions.*

**AUTHORS’ REONSE:** Thank you for your good suggestion. Following the reviewer’s suggestion we have added a flow chart of methodology, as show in Fig. 1 in the revised manuscript.

*Why the authors choose Weihe River basin as a case study? Are there any unique features of the study region when compared to other alternative rivers?*

**AUTHORS’ REONSE:** The nonstationarity of annual runoff in Weihe River basin has been shown to be very significant (Lin et al., 2012; Xiong et al., 2014). The previous studies have demonstrated that the climate change and human activities play an important role in annual runoff changes. When compared to other alternative rivers, the nonstationarity mode of low flows in the study region is so complex that it is difficult to be identified due to the influence of various factors. This feature aroused our interest in choosing the study area. We try to demonstrate that the nonstationarity of low flows in this basin is caused by multiple factors and more effective analysis model should incorporate not only a single climate index or human activity indices but also the other climate indices and catchment condition indices. We have clarified this point.

## References

Arora, V. K.: The use of the aridity index to assess climate change effect on annual runoff, *Journal of Hydrology*, 265, 164-177, 2002.

Chen, X., Zhang, L., Xu, C. Y., Zhang, J., and Ye, C.: Hydrological Design of

Nonstationary Flood Extremes and Durations in Wujiang River, South China: Changing Properties, Causes, and Impacts, Mathematical Problems in Engineering, 2013, (2013-6-2), 2013, 211-244, 2013.

Cheng, L. and AghaKouchak, A.: Nonstationary precipitation Intensity-Duration-Frequency curves for infrastructure design in a changing climate, Sci Rep, 4, 7093, 2014.

Du, T., Xiong, L., Xu, C.-Y., Gippel, C. J., Guo, S., and Liu, P.: Return period and risk analysis of nonstationary low-flow series under climate change, Journal of Hydrology, 527, 234-250, 2015.

Gilroy, K. L. and Mccuen, R. H.: A nonstationary flood frequency analysis method to adjust for future climate change and urbanization, Journal of Hydrology, 414-415, 40-48, 2012.

Gu, X., Zhang, Q., Singh, V. P., Chen, X., and Liu, L.: Nonstationarity in the occurrence rate of floods in the Tarim River basin, China, and related impacts of climate indices, Global & Planetary Change, 142, 1-13, 2016.

Gu, X., Zhang, Q., Singh, V. P., and Shi, P.: Changes in magnitude and frequency of heavy precipitation across China and its potential links to summer temperature, Journal of Hydrology, 547, 2017a.

Gu, X., Zhang, Q., Singh, V. P., and Shi, P.: Non-stationarities in the occurrence rate of heavy precipitation across China and its relationship to climate teleconnection patterns, International Journal of Climatology, 2017b.

Gu, X., Zhang, Q., Singh, V. P., and Shi, P.: Nonstationarity in timing of extreme precipitation across China and impact of tropical cyclones, Global & Planetary Change, 149, 153-165, 2017c.

Jiang, C., Xiong, L., Guo, S., Xia, J., and Xu, C. Y.: A process-based insight into nonstationarity of the probability distribution of annual runoff, Water Resources Research, 2017.

Jiang, C., Xiong, L., Wang, D., Liu, P., Guo, S., and Xu, C.-Y.: Separating the impacts of climate change and human activities on runoff using the Budyko-type equations with time-varying parameters, Journal of Hydrology, 522, 326-338, 2015.

Jiang, C., Xiong, L., Xu, C. Y., and Guo, S.: Bivariate frequency analysis of nonstationary low-flow series based on the time-varying copula, Hydrological Processes, 29, 1521-1534, 2014.

Kwon, H.-H., Brown, C., and Lall, U.: Climate informed flood frequency analysis and prediction in Montana using hierarchical Bayesian modeling, Geophysical Research Letters, 35, 2008.

López, J. and Francés, F.: Non-stationary flood frequency analysis in continental Spanish rivers, using climate and reservoir indices as external covariates, Hydrology and Earth System Sciences, 17, 3189-3203, 2013.

Lin, Q. C., Huai-En, L. I., and Xi-Jun, W. U.: Impact of Water Diversion of Baojixia Irrigation Area to the Weihe River Runoff, Yellow River, 2012.

Liu, D., Guo, S., Lian, Y., Xiong, L., and Chen, X.: Climate-informed low-flow frequency analysis using nonstationary modelling, Hydrological Processes, 29, 2112-2124, 2015.

Liu, J., Zhang, Q., Singh, V. P., and Shi, P.: Contribution of multiple climatic variables and human activities to streamflow changes across China, *Journal of Hydrology*, 545, 2017.

Milly, P. C. D., Betancourt, J., Falkenmark, M., Hirsch, R. M., Kundzewicz, Z. W., Lettenmaier, D. P., and Stouffer, R. J.: Stationarity Is Dead: Whither Water Management?, *Science*, 319, 573-574, 2008.

Mondal, A. and Mujumdar, P. P.: Modeling non-stationarity in intensity, duration and frequency of extreme rainfall over India, *Journal of Hydrology*, 521, 217-231, 2015.

Salas, J. D.: Analysis and modeling of hydrologic time series, *Handbook of Hydrology*, 1993. 1993.

Shahabul Alam, M., Nazemi, A., and Elshorbagy, A.: Quantifying the climate change-induced variations in Saskatoon's Intensity-Duration-Frequency curves using stochastic rainfall generators and K-nearest neighbors, 2014.

Smakhtin, V. U.: Low flow hydrology: a review, *Journal of Hydrology*, 2001.

Tang, Y., Xi, S., Chen, X., and Lian, Y.: Quantification of Multiple Climate Change and Human Activity Impact Factors on Flood Regimes in the Pearl River Delta of China, *Advances in Meteorology*, 2016, 1-11, 2015.

Villarini, G., Smith, J. A., and Napolitano, F.: Nonstationary modeling of a long record of rainfall and temperature over Rome, *Advances in Water Resources*, 33, 1256-1267, 2010.

Xiong, L., Du, T., Xu, C. Y., Guo, S., Jiang, C., and Gippel, C. J.: Non-Stationary Annual Maximum Flood Frequency Analysis Using the Norming Constants Method to Consider Non-Stationarity in the Annual Daily Flow Series, *Water Resources Management*, 29, 3615-3633, 2015.

Xiong, L., Jiang, C., and Du, T.: Statistical attribution analysis of the nonstationarity of the annual runoff series of the Weihe River, *Water Science & Technology*, 70, 939-946, 2014.

Yan, L., Xiong, L., Liu, D., Hu, T., and Xu, C. Y.: Frequency analysis of nonstationary annual maximum flood series using the time-varying two-component mixture distributions, *Hydrological Processes*, 2016.

Yang, H. and Yang, D.: Derivation of climate elasticity of runoff to assess the effects of climate change on annual runoff, *Water Resources Research*, 47, 197-203, 2011.

Yang, H. and Yang, D.: Evaluating attribution of annual runoff change: according to climate elasticity derived using Budyko hypothesis, *Egu General Assembly*, 15, 14029, 2013.

Zhang, Q., Gu, X., Singh, V. P., and Xiao, M.: Flood frequency analysis with consideration of hydrological alterations: Changing properties, causes and implications, *Journal of Hydrology*, 519, 803-813, 2014.

Zhang, Q., Gu, X., Singh, V. P., Xiao, M., and Chen, X.: Evaluation of flood frequency under non-stationarity resulting from climate indices and reservoir indices in the East River basin, China, *Journal of Hydrology*, 527, 565-575, 2015.

Zhang, S., Yang, H., Yang, D., and Jayawardena, A. W.: Quantifying the effect of

vegetation change on the regional water balance within the Budyko framework, Geophysical Research Letters, 43, n/a-n/a, 2015.

## -Referee#2-

*General Comment This work covered an interesting topic. It is qualified for HESS after a minor revision. Authors incorporated multiple variables into time-varying model by GLM, and called this a nonstationary mode considering TCCCs. They calculated and compared AIC of this mode with that of the stationary mode and the nonstationary mode with a single covariate in two stations in Weihe. Then they concluded this TCCCs nonstationary mode was the optimal one for nonstationary low flow frequency analysis in Weihe.*

**AUTHORS' REPONSE:** Thank you for your positive evaluation and a good summary of the paper.

*It's a pity that they did a lot of work without clearly stating their motivation. Authors first raised an issue in review that the previous studies in low flow failed to provide a link between hydrological process and frequency analysis, and this made it difficult for tracing the origins of low flow change. While readers might think they intend to trace these origins (which was also hinted by the title), they defended that "the goal of this study is to develop a nonstationary low-flow frequency analysis framework". It is better for them to keep consistent in the whole introduction section.*

**AUTHORS' REPONSE:** Thank you for your comments and the good suggestion. This is also pointed out by reviewer 1. Following the reviewer's advice, we have also better stated our study motivation as following.

“To our knowledge, compared with the nonstationary flood frequency analysis, the studies on the nonstationary frequency analysis of low-flow series are not very extensive because of incomplete knowledge of low flow generation (Smakhtin, 2001). Most of these studies explain nonstationarity of low-flow series only by using climatic indicators or a single indicator of human activity. However, the indicators of catchment conditions (e.g. recession rate) related to physical hydrological processes have seldom been attached in nonstationary modeling of low flow series. This lack of linking with hydrological processes makes it impossible to accurately quantify the contributions of influencing factors for the nonstationarity of low flow series, and such a scientific demand for tracing the sources of nonstationarity of low-flow series and qualifying their contributions motivated the present study...” [Lines 100-109]

We have also explicitly defined and stated the study objectives in the 5<sup>th</sup> paragraph of the Introduction Section, as follows:

“The goal of this study is to trace origins of nonstationarity in low flows through developing a nonstationary low-flow frequency analysis framework with the consideration of the time-varying climate and catchment conditions (TCCCs) and

human activity (HA). In this framework, the climate and catchment conditions are quantified using the eight indices, i.e., meteorological variables (total precipitation  $P$ , mean frequency of precipitation events  $\lambda$ , temperature  $T$  and potential evapotranspiration  $ET$ ), basin storage characteristics (base-flow index  $BFI$ , recession constant  $K$ ) and aridity indexes (climate aridity index  $AI_{ET}$ , the recession-related aridity index  $AI_K$ ). The specific objectives of this study are: (1) to find the most important index to explain the nonstationarity of low-flow series; (2) to determine the best subset of TCCCs indices and/or human activity indices (i.e., population  $POP$ , irrigation area  $IAR$ , and gross domestic product  $GDP$ ) for final model through stepwise selection method to identify nonstationary mode of low-flow series; and (3) to quantify the contribution of selected explanatory variables to the nonstationarity.” [Lines 131-142]

*Besides, to better show the advantage of this framework, which was composed of the time-varying and GLM method, they should compare it with other models using only climatic indicators or a single indicator of human activity, just as they mentioned in the review, not just the mode with either  $AI_K$  or  $BFI$  as the explanatory variable.*

**AUTHORS’ REONSE:** Thank you for the comment. Our study had included the model with climate indicators. But, indeed, the model with a single indicator of human activity (e.g. irrigation, population, GDP as mentioned by the first reviewer) was not involved in the original submission. Thus to address this comment, the main and supplementary texts have been revised to compare the nonstationary mode considering TCCCs with the nonstationary mode considering human activity (irrigation, population, GDP), as also stated in the reply to reviewer 1. The process of their change with time has been presented (see Fig. 5 in the revised manuscript). The Pearson correlation coefficients between low-flow series and these indices have been presented (see Fig. 6 in the revised manuscript). The models (M2b, M5, and M6, as described in Table 2 in the revised manuscript) are added. The summary of their results has been presented in Table 5 in the revised manuscript. All new results have been shown in Figs. 7, 8, 9, 10 and 11 in the revised manuscript. Statements in the Results Section have been added and revised, as shown in the revised manuscript with tracked changes.

*In addition, there are some mistakes and improper statements in this paper; outlines of methods and results are unclear, and the discussion is weak. It is better for authors to put together contents of results and discussion, and further discuss their results and compared with other related works.*

**AUTHORS’ REONSE:** Thank you for your comment. The mistakes and improper statements have been carefully checked and corrected in the revised version; to clarify methods, a flow chart of methodology and a table which summarizes the explanatory variables have been added; and we have revised the contents of results and discussion, following the reviewer’s good suggestion. The revised manuscript has included further discussion of results and comparison with other related works as following:

“Overall, the causes of nonstationarity in category for two gauging stations have no clear difference, but have some differences in the relative importance. As shown in Table 5, when modeling the low-flow series of Huaxian using TCCCs variables, the optimal model (M4) preferred the variables are related to recession process; however, for Xianyang, the preferred variables are related to temperature. The reason for this may be that as a downstream station, Huaxian station suffers more intensive human activity, so that the importance of temperature change to the low-flow change is reduced, and meanwhile the importance of streamflow recession (related to the capability of water storage) change is enhanced.” [Lines 493-501]

“The related researches (Jiang et al., 2015; Yang and Yang, 2011; Yang and Yang, 2013; Zhang et al., 2015) have applied the Budyko framework to analyze the impacts of climate change and/or human activity on annual runoff. Indeed, for annual runoff, the Budyko framework is a good method because it used the mean annual water-energy balance equation to consider generation process of total runoff. Unfortunately, to our knowledge, there is a lack of equation derived from basic physics laws for generation process of low flows. Therefore, we emphasize the importance of TCCCs variables to modeling of low-flow nonstationarity.” [Lines 507-513]

*Specific Comment The logic of review in the introduction is not smooth. Some references mentioned in the paragraph starting from Line 52, such as Lars Gottschalk's work, were badly concluded and they'd better be put in the next paragraph.*

**AUTHORS' REONSE:** Thank you for pointing out this and for your good suggestion. To address your comment, we have revised the introduction as mentioned above.

*A flow chart of methodology is needed.*

**AUTHORS' REONSE:** This is a good point. To address your comment, we have added it (Fig. 1 in the revised manuscript).

*Line 127 Meaning of this sentence is obscure.*

**AUTHORS' REONSE:** The sentence has been revised as following: “The distribution type used to build the nonstationary model is outlined”

*Further explanation for the selection of 8 candidate variables is needed.*

**AUTHORS' REONSE:** Thank you for the comment. To address this comment, the 1st paragraph of ‘Section 2.3 Candidate explanatory variables’ has been revised. And the reason for the selection of 8 candidate variables has been listed in Table 3 in the revised manuscript.

*Indices more related to irrigation, like irrigation area, need to be considered, since (Line278) In the Weihe basin, the impacts of agricultural irrigation on runoff have been found to be significant.*

**AUTHORS' REONSE:** Thank you for the comment. Following reviewer's suggestions, we have included this index (irrigation area) as mentioned above.

*Both those 8 explanatory variables and data resources can be summarized in two tables.*

**AUTHORS' REONSE:** This is a good point. To address this comment, we have revised the text and added Table 3 in the revised manuscript.

*I don't see much use in Figure 2.*

**AUTHORS' REONSE:** Thank you for the comment. Following your suggestion, the Figure has been deleted in the revised manuscript.

*Why do you need to study all the series from AM1, 7, 15 to 30?*

**AUTHORS' REONSE:** The main reason for including four series is to investigate whether the time scale of the series affects the nonstationary mode. As shown in Figure 7 (the revised manuscript), the effect of time scale is existed but limited. In response to this good comment, we have revised the part of the Multiple Covariate Analysis Section to focus on the  $AM_{30}$  series.

*In some subplans in Figure 8, AIC of either M2 or M3 is worse than M1. What is the probable cause? The conclusion in Line 391 cannot be directly generated from Figure8.*

**AUTHORS' REONSE:** We have explained that this phenomenon mainly appears in the  $AM_1$  and  $AM_7$  series.  $AM_1$  and  $AM_7$  series are more vulnerable, which means that multiple causes can affect them. The nonstationary mode with one or two physical explanatory variables (M2 or M3) cannot work well for  $AM_1$  and  $AM_7$ . However, the overall decreased trend caused by multiple factors is consistent with the nonstationary mode with time (M1).

*What is the impact of location difference on the different AIC results in two stations? Needs to add discussion.*

**AUTHORS' REONSE:** This is a good point. Following the reviewer's suggestion, we have added a supplemental part to the discussion section (see lines 482-489 in the revised manuscript).

*The standard of selecting M4 variables with stepwise selection method needs to be further clarified.*

**AUTHORS' REONSE:** Following the reviewer's suggestion, we have clarified the standard of the models' variables using Fig. 1 in the revised manuscript.

*Table5 and 6 can be merged into one table.*

**AUTHORS' REONSE:** Agree, corrected.

*Formula 2, no need to put "i=" on the top*

**AUTHORS' REONSE:** Corrected.

*Table2, add explanation for parameters down below the table*

**AUTHORS' REONSE:** Corrected.

*The definition, reason of selection, and formula of 8 indices should be listed in a table.*

**AUTHORS' REONSE:** Corrected.

*Line228, 234, 242 add blank space before the paragraph (need to check in the whole paper)*

**AUTHORS' REONSE:** Corrected.

*Line298 slash tag between “n” and “day” is missing (check the whole paper)*

**AUTHORS' REONSE:** Corrected.

*Line304 mistake in time tense*

**AUTHORS' REONSE:** Corrected.

*Line388 incomplete sentence*

**AUTHORS' REONSE:** Corrected.

*Figure1 mark the location of Weihe in the map of China with a rectangular frame*

**AUTHORS' REONSE:** Corrected.

*Figure3 adding R*

**AUTHORS' REONSE:** Corrected.

*Figure 3 &4 lines are too thick*

**AUTHORS' REONSE:** Corrected.

*Figure5&6 differences among colors are too delicate to be seen*

**AUTHORS' REONSE:** Corrected.

*Table 3 &4 add division lines among rows of different stations*

**AUTHORS' REONSE:** Corrected.

*Mistake in references, year of “Bivariate frequency analysis of nonstationary low-flow series based on the time-varying copula” was 2015*

**AUTHORS' REONSE:** Thank you for pointing out this. We have corrected this.

## References

Jiang, C., Xiong, L., Wang, D., Liu, P., Guo, S., and Xu, C.-Y.: Separating the impacts of climate change and human activities on runoff using the Budyko-type equations with time-varying parameters, *Journal of Hydrology*, 522, 326-338, 2015.

Smakhtin, V. U.: Low flow hydrology: a review, *Journal of Hydrology*, 2001.

Tang, Y., Xi, S., Chen, X., and Lian, Y.: Quantification of Multiple Climate Change and Human Activity Impact Factors on Flood Regimes in the Pearl River Delta of China, *Advances in Meteorology*, 2016, 1-11, 2015.

Yang, H. and Yang, D.: Derivation of climate elasticity of runoff to assess the effects of climate change on annual runoff, *Water Resources Research*, 47, 197-203, 2011.

Yang, H. and Yang, D.: Evaluating attribution of annual runoff change: according to climate elasticity derived using Budyko hypothesis, *Egu General Assembly*, 15, 14029, 2013.

Zhang, S., Yang, H., Yang, D., and Jayawardena, A. W.: Quantifying the effect of vegetation change on the regional water balance within the Budyko framework, *Geophysical Research Letters*, 43, n/a-n/a, 2015.

Thanks again to the editor and the two reviewers for providing professional and insightful comments and advices which have significantly improved the revised version of the manuscript.

Sincerely,

Bin Xiong, Lihua Xiong, Jie Chen, Chong-Yu Xu, Lingqi Li

1                   **Multiple Causes of Nonstationarity in the Weihe Annual Low Flow Series**

2                   Bin Xiong<sup>1</sup>, Lihua Xiong<sup>1\*</sup>, Jie Chen<sup>1</sup>, Chong-Yu Xu<sup>1, 2</sup>, Lingqi Li<sup>1</sup>

3                   1 State Key Laboratory of Water Resources and Hydropower Engineering Science, Wuhan

4                   University, Wuhan 430072, P.R. China

5                   2 Department of Geosciences, University of Oslo, P.O. Box 1022 Blindern, N-0315 Oslo,

6                   Norway

7

8                   *\* Corresponding author:*

9                   Lihua Xiong, PhD, Professor

10                   State Key Laboratory of Water Resources and Hydropower Engineering Science

11                   Wuhan University, Wuhan 430072, P.R. China

12                   E-mail: xionglh@whu.edu.cn

13                   Telephone: +86-13871078660

14                   Fax: +86-27-68773568

16 **Abstract:**

17 Under the background of global climate change and local anthropogenic activities, multiple  
18 driving forces have introduced ~~a variety of various~~ non-stationary components into low-flow series.  
19 This has led to a high demand on low-flow frequency analysis that considers nonstationary  
20 conditions for modeling. In this study, ~~through~~ a nonstationary ~~frequency analysis~~ framework ~~of~~  
21 ~~low flow frequency analysis has been developed on basis of with~~ the Generalized Linear Model  
22 (GLM) to consider time-varying distribution parameters. ~~In GLMs, the candidate multiple~~  
23 ~~explanatory variables whereas incorporated to explain the time varying the variation in low-flow~~  
24 ~~distribution~~ parameters. ~~These variables~~ are comprised of ~~the three indices of human activities (i.e.,~~  
25 ~~population POP, irrigation area IAR, and gross domestic product GDP) and~~ the eight measuring  
26 indices of the climate and catchment conditions ~~in low flow generation~~, (i.e., total precipitation  $P$ ,  
27 mean frequency of precipitation events  $\lambda$ , temperature  $T$ , potential evapotranspiration  $ET$ , climate  
28 aridity index  $AI_{ET}$ , base-flow index  $BFI$ , recession constant  $K$  and the recession-related aridity  
29 index  $AI_K$ ). This framework was applied to ~~model~~ the annual minimum flow series of both  
30 Huaxian and Xianyang gauging stations in the Weihe River, China. ~~Stepwise regression analysis~~  
31 ~~was performed to obtain the best subset of those candidate explanatory variables for the final~~  
32 ~~optimum model.~~ The results ~~from stepwise regression for the optimal explanatory variables~~ show  
33 that ~~the inter annual variability in the variables of those selected best subsets the variables~~

34 related to irrigation, recession, temperature and precipitation plays an important role in modeling  
35 annual low flow series. Specifically, analysis of annual minimum 30-day flow in Huaxian shows  
36 that  $AI_K$  is of the highest relative importance among the optimal variables, followed by *IAR*, *BFI*  
37 and  $AI_{ET}$ , and nonstationary GA distribution model with these optimal variables has an AIC  
38 value of 207.0, while the AIC values of other models just with  $AI_K$  or time as explanatory variables  
39 or without any variable are 217.4, 225.5, 232.3, respectively.  $AI_K$  is of the highest relative  
40 importance among the best subset of eight candidates, followed by *BFI* and  $AI_{ET}$ . We conclude  
41 that ~~The~~ incorporation of multiple indices related to low-flow generation permits tracing  
42 various driving forces. The established link in nonstationary analysis will be beneficial to ~~predict~~  
43 ~~analyze~~ future occurrences of low-flow extremes in similar areas.

44 **Keywords:** Climate Change; Streamflow Recession; Multiple Factors; Nonstationarity;  
45 Low-flow Frequency Analysis;

46

## 47 1. Introduction

48 Low flow is defined as the ‘flow of water in a stream during prolonged dry weather’ (WMO,  
49 1974). Yu et al. (2014) quantitatively described a low flow event as a segment of hydrograph  
50 during a period of dry weather with discharge values below a preset (relatively small) threshold.  
51 According to WMO (2009), annual minimum flows averaged over several days can be used to

52 measure low flows. During low-flow periods, the magnitude of river flow will greatly restrict its  
53 various functions (e.g. providing water supply for production and living, diluting waste water,  
54 ensuring navigation, meeting ecological water requirement). Therefore, The investigation of the  
55 magnitude and frequency of low flows is of primary importance for engineering design and water  
56 resources management (Smakhtin, 2001). For In recent years, low flows, as an important part of  
57 river flow regime, have been attracting the an increasing attentions of hydrologists and ecologists,  
58 due to in the context of the significant impacts of climate change and human activities ~~on most~~  
59 ~~functions (e.g. providing water supply for production and living, diluting waste water, ensuring~~  
60 ~~navigation, meeting ecological water requirement) of river flow during low flow periods.~~  
61 (Bradford and Heinonen, 2008; Du et al., 2015; Kam and Sheffield, 2015; Kormos et al., 2016; Liu  
62 et al., 2015; Sadri et al., 2015; Smakhtin, 2001; WMO, 2009). In general, under the impact of a  
63 changing environment, combinations of multiple factors, such as precipitation change, temperature  
64 change, irrigation area change and construction of reservoirs, can drive various patterns of  
65 streamflow changes (Liu et al., 2017; Tang et al., 2015). Unfortunately, when subjected to a variety  
66 of influencing forces, low flow is more vulnerable than high flow or mean flow. Therefore, it is a  
67 pretty important issue in hydrology to identify low-flow changes, track multiple driving factors  
68 and quantify their contributions from the perspective of hydrological frequency analysis.  
69

70       In hydrological analysis and design, conventional frequency analysis estimates the statistics  
71       of a hydrological time series based on recorded data with the stationary hypothesis which means  
72       that this series is “free of trends, shifts, or periodicity (cyclicity)” (Salas, 1993). However, global  
73       warming and human forces have changed climate and catchment conditions in some regions.  
74       Time-varying climate and catchment conditions can affect all aspects of the flow regime, i.e.  
75       changing the frequency and magnitude of floods, altering flow seasonality, and modifying the  
76       characteristics of low flows, etc. The hypothesis of stationarity has been suspected (Milly et al.,  
77       2008). If this problematic method is still used, the frequency analysis may lead to high estimation  
78       error and costly in hydrological design. Therefore, considerable literatures have introduced the  
79       concept of hydrologic nonstationarity into analysis of various hydrological variables, such as  
80       annual runoff (Arora, 2002; Jiang et al., 2017; Jiang et al., 2015; Liu et al., 2017; Xiong et al.,  
81       2014; Yang and Yang, 2013), flood (Chen et al., 2013; Gilroy and Mccuen, 2012; Gu et al., 2016;  
82       Kwon et al., 2008; López and Francés, 2013; Tang et al., 2015; Xiong et al., 2015b; Yan et al.,  
83       2016; Zhang et al., 2014; Zhang et al., 2015), low flow (Du et al., 2015; Jiang et al., 2014; Liu et  
84       al., 2015), precipitation (Cheng and AghaKouchak, 2014; Gu et al., 2017a, b, c; Mondal and  
85       Mujumdar, 2015; Villarini et al., 2010) and so on. Compared with the literatures on annual runoff,  
86       floods and precipitation, the literatures on the nonstationary analysis of low flow are very relatively  
87       limited.

88 Previous hydrological literatures on frequency analysis of nonstationary ~~low-flow~~  
89 hydrological series mainly focus on two aspects: development of nonstationary method and  
90 exploration of covariates reflecting changing environments. Strupczewski et al. (2001) presented  
91 the method of time-varying moment which assumes that the hydrological variable of interest obeys  
92 a certain distribution type, but its moments change over time. The method of time-varying moment  
93 was modified to be the method of time-varying parameter values for the distribution representative  
94 of hydrologic data (Richard et al., 2002). Villarini et al. (2009) presented this method using the  
95 Generalized Additive Models for Location, Scale, and Shape Parameters (GAMLSS) (Rigby and  
96 Stasinopoulos, 2005), a flexible framework to assess nonstationary time series. The time-varying  
97 parameter method can be extended to the physical covariate analysis by replacing time with any  
98 others physical covariates (Du et al., 2015; Jiang et al., 2014; Kwon et al., 2008; López and  
99 Francés, 2013; Liu et al., 2015; Villarini et al., 2010; Villarini and Strong, 2014). For example,  
100 Jiang et al. (2014) used reservoir index as an explanatory variables based on the time-varying  
101 copula method for bivariate frequency analysis of nonstationary low-flow series in Hanjiang River,  
102 China. Du et al. (2015) took precipitation and air temperature as the explanatory variables to  
103 explain the inter-annual variability in low flows of Weihe River, China. Liu et al. (2015) took Sea  
104 Surface Temperature in Nino3 region, the Pacific Decadal Oscillation, the sunspot number (3 years  
105 ahead), the winter areal temperature and precipitation as the candidate explanatory variables to

106 explain the inter-annual variability in low flows of Yichang station, China. Kam and Sheffield  
107 (2015) ascribed the increasing inter-annual variability of low flows over the eastern United States  
108 to North Atlantic Oscillation and Pacific North America.

109 ~~Low flows are more vulnerable to influences of climate change and human activities than~~  
110 ~~high flows. However, To our knowledge,~~ compared with the nonstationary flood frequency  
111 analysis, the studies on the nonstationary frequency analysis of low-flow series is not very  
112 extensive because of incomplete knowledge of low flow generation (Smakhtin, 2001). Most of  
113 these studies explain nonstationarity of low-flow series only by using climatic indicators or a  
114 single indicator of human activity. However, the indicators of catchment conditions (e.g. recession  
115 rate) related to physical hydrological processes have seldom been attached in nonstationary  
116 modeling of low flow series. ~~This leads to lack of linking with hydrological process, which in~~  
117 ~~turn would exclude further analysis, such as accurately tracing origins of change in low flow~~  
118 ~~series~~ This lack of linking with hydrological processes makes it impossible to accurately quantify  
119 the contributions of influencing factors for the nonstationarity of low flow series, and such a  
120 scientific demand for tracing the sources of nonstationarity of low-flow series and qualifying their  
121 contributions motivated the present study. The knowledge of low-flow generation has been  
122 increased by efforts of hydrologists, which can help develop physical covariates to address  
123 nonstationarity. Low flows generally originate from groundwater or other delayed outflows

124 (Smakhtin, 2001; Tallaksen, 1995). Their generation relates to both an extended dry weather  
125 period (leading to a climatic water deficit) and complex hydrological processes which determine  
126 how these deficits propagate through the vegetation, soil and groundwater system to streamflow  
127 (WMO, 2009). Thus, not only climate condition~~s~~ drivers (e.g. potential evaporation exceeds  
128 precipitation), but also catchment condition~~s~~ drivers (e.g. the faster hydrologic response rate to  
129 precipitation) can cause low flows.

130 The significant factors such as precipitation, temperature, evapotranspiration, streamflow  
131 recession, large-scale teleconnections and human forces may play important roles in influencing  
132 low-flow generation (Botter et al., 2013; Giuntoli et al., 2013; Gottschalk et al., 2013; Jones et al.,  
133 2006; Kormos et al., 2016; Roderick et al., 2013; Sadri et al., 2015). Gottschalk et al. (2013)  
134 presented a derived low flow probability distribution function with climate and catchment  
135 characteristics parameters (i.e., the mean length of dry spells  $\lambda^{-1}$  and recession constant of  
136 streamflow  $K$ ) as its distribution parameters. Botter et al. (2013) derived “a measurable index”  
137 ( $\lambda^{-1}/K$ ) which can be used for discriminating erratic river flow regimes from persistent river flow  
138 regimes. Recently, in Van Loon and Laaha (2015) used climate and catchment characteristics (e.g.  
139 the duration of dry spells in precipitation and the base flow index) to explain the duration and  
140 deficit of hydrological drought event and offered a further understanding of low-flow generation.  
141 These studies indicated that climate and catchment conditions play an important role in producing

142 low flows.

143 The goal of this study is to trace origins of nonstationarity in low flows through developing a  
144 nonstationary low-flow frequency analysis framework with the consideration of the time-varying  
145 climate and catchment conditions (TCCCs) and human activity (HA). The goal of this study is to  
146 develop a nonstationary low flow frequency analysis framework with the consideration of the  
147 time varying climate and catchment conditions (TCCCs). In this framework, the climate and  
148 catchment conditions are quantified using the eight indices, i.e., meteorological variables (total  
149 precipitation  $P$ , mean frequency of precipitation events  $\lambda$ , temperature  $T$  and potential  
150 evapotranspiration  $ET$ ), basin storage characteristics (base-flow index  $BFI$ , recession constant  
151  $K$ ) and aridity indexes (climate aridity index  $AI_{ET}$ , the recession-related aridity index  $AI_K$ ).

152 The specific objectives of this study are: (1) to find the most important index to explain the  
153 nonstationarity of low-flow series; (2) to determine the best subset of TCCCs indices and/or  
154 human activity indices (i.e., population  $POP$ , irrigation area  $IAR$ , and gross domestic product  $GDP$ )  
155 for final model through stepwise selection method to identify nonstationary mode of low-flow  
156 series; and (3) to quantify the contribution of selected explanatory variables to the nonstationarity.

157 The non-stationary frequency analysis with TCCCs developed in this study is able to give the trace  
158 of nonstationary low flow drivers and to estimate the contribution of each driver to the change in  
159 low flow series.

160 This paper is organized as follows. Section 2 describes the methods. ~~We describe the Weihe~~  
161 River basin and available data sets used in this study ~~are described~~ in Section 3, followed by a  
162 presentation of the results and discussion in Section 4. Section 5 summarizes the main conclusions.

163 **2 Methodology**

164 The flowchart of how to organize the nonstationary low-flow frequency analysis framework  
165 is shown in Fig. 1. The whole process is divided into three steps. The first step is preliminary  
166 analysis, including the graphical presentation of both explanatory variables and low-flow series,  
167 the statistical test for nonstationarity and the correlations between each explanatory variable and  
168 each low-flow series. The second step is single covariate analysis for the most important  
169 explanatory variable. The third step is multiple covariate analysis for the optimal combination. We  
170 use a low-flow frequency analysis model and stepwise regression method to accomplish the last  
171 two steps. In this the following sub-sections, first, the low-flow frequency analysis model is  
172 constructed based on the nonstationary probability distributions method, in which distribution  
173 parameters serving as response variables can vary as functions of explanatory variables. Second,  
174 ~~the candidate distributions are described to determine the different types of nonstationary~~  
175 ~~frequency curves. the distribution types used to build the nonstationary model are outlined.~~ Then,  
176 the ~~eight~~ candidate explanatory variables ~~related to the time-varying climate and catchment~~

177 ~~conditions (TCCCs) and human activity (HA) are clarified presented to incorporate time varying~~  
178 ~~climate and catchment conditions (TCCCs) into distribution models for the nonstationary~~  
179 ~~frequency analysis~~. Finally, estimation of model parameters and selection of models are illustrated.

180 <Figure 1>

181 **2.1 Construction of the low-flow nonstationary frequency analysis model**

182 Generally, a nonstationary frequency analysis model can be established based on the  
183 time-varying distribution parameters method (Du et al., 2015; López and Francés, 2013; Liu et al.,  
184 2015; Richard et al., 2002; Villarini and Strong, 2014). For the nonstationary probability  
185 distribution  $f_Y(Y_t|\boldsymbol{\theta}^t)$ , let  $Y_t$  be a random variable at time  $t (t=1,2,\dots,N)$  and vector  
186  $\boldsymbol{\theta}^t = [\theta_1^t, \theta_2^t, \dots, \theta_m^t]$  be the time-varying parameters. The number of parameters  $m$  in hydrological  
187 frequency analysis is generally limited to three or less. The function relationship between the  $k^{th}$   
188 parameter  $\theta_k^t$  and the multiple explanatory variables is expressed as follows:

189 
$$g_k(\theta_k^t) = h_k(x_1^t, x_2^t, \dots, x_n^t) \quad (1)$$

190 where  $x_1^t, x_2^t, \dots, x_n^t$  are explanatory variables;  $n$  is the number of explanatory variables;  $g_k(\cdot)$   
191 is the link function which ensures the compliance with restrictions on the sample space and is  
192 usually set to natural logarithm for the given negative predictions;  $h_k(\cdot)$  is the function for  
193 nonstationary modeling. The theory of Generalized Linear Model (Dobson and Barnett, 2012) is  
194 used to build function relationships between distribution parameters and their explanatory

195 variables. In GLMs, the response relationship can be generally expressed as

196

$$g_k(\theta_k) = \alpha_{0k} + \sum_{i=1} \alpha_{ik} x_i^t \quad (2)$$

197 where  $\alpha_{ik}$  ( $i = 0, 1, 2, \dots, n, k = 1, \dots, m$ ) are the GLM parameters.

198 In order to give a further nonstationary analysis is compare the nonstationary models constructed  
199 by various combinations of explanatory variables, Eq. (2) is modified in this study using  
200 dimensionless method for the standard GLM parameters. The value of  $\theta_k^t$  could be assumed to be  
201 equal to its mean ( $\bar{\theta}_k$ ) when all explanatory variables are equal to their mean ( $\bar{x}_i$ ), i.e.,

202

$$\theta_k' (x_1^t = \bar{x}_1, x_2^t = \bar{x}_2, \dots, x_n^t = \bar{x}_n) = \bar{\theta}_k \quad (3)$$

203 Eq. (2) is then modified as

$$g_k \left( \frac{\theta_k^t}{\bar{\theta}_k} \right) = \beta_{0k} + \sum_{i=1}^n \beta_{ik} z_i^t$$
$$z_i^t = \frac{x_i^t - \bar{x}_i}{s_i}, \quad i = 1, 2, \dots, n \quad (4)$$
$$\beta_{0k} = g_k \left( \frac{\theta_k^t}{\bar{\theta}_k} \middle| \theta_k^t = \bar{\theta}_k \right) = g_k(1)$$

204 where  $z_i^t$  is normalized explanatory variables;  $s_i$  is the standard deviation of  $x_i^t$ ;  
205  $\beta_{ik}$  ( $i = 1, 2, \dots, n, k = 1, \dots, m$ ) are the standard GLM parameters. Let the link function  $g_k(\cdot)$  be the  
206 natural logarithmic function  $\ln(\cdot)$  and  $\theta_l^t$  be the distribution parameter in  $[\theta_1^t, \theta_2^t, \dots, \theta_m^t]$  with  
207 most significant change, the degree of nonstationarity in low flow series can be defined as  
208  $\ln(\theta_l^t) - \ln(\bar{\theta}_l)$ . Then, the contribution  $c_i^t$  of each explanatory variable  $x_i^t$  to  $\ln(\theta_l^t) - \ln(\bar{\theta}_l)$

210 could be defined as

211

$$c_i^t = \beta_{il} \frac{x_i^t - \bar{x}_i}{s_i} \quad (5)$$

212 **2.2 Candidate distribution functions**

213 We need to select the form of probability distribution  $f_Y(\cdot)$  to determine what type of  
214 nonstationary frequency curves will be produced. Various probability distributions have been  
215 compared or suggested in modeling of low-flow series (Du et al., 2015; Hewa et al., 2007; Liu et  
216 al., 2015; Matalas, 1963; Smakhtin, 2001). An extensive overview of distribution functions for low  
217 flow is given in Tallaksen et al. (2004). Following these recommendations, we consider five  
218 distributions, i.e. Pearson-III (PIII), Gamma (GA), Weibull (WEI), Lognormal (LOGNO) and  
219 Generalized Extremes Value (GEV) as candidates in this study (Table 1). In the case of Pearson-III  
220 distribution, considering that the parameter  $\theta_3$  of Pearson-III as lower bound should approach  
221 zero and the parameter  $\theta_3$  of GEV is quite sensitive and difficult to be estimated, we assume  
222 them to be constant in this study.

223 **2.3 Candidate explanatory variables**

224 We look for variables  $x_1^t, x_2^t, \dots, x_n^t$  that can explain parts of the variations in distribution  
225 parameters  $\theta'$ . From the perspective of low-flow generation, the dependency between low-flow  
226 regime and both climate and catchment conditions has been presented by previous studies (Botter

227 et al., 2013; Gottschalk et al., 2013; Van Loon and Laaha, 2015). We focus on eight measuring  
228 indices: total precipitation, mean frequency of precipitation events, temperature, potential  
229 evapotranspiration, climate aridity index, base-flow index, recession constant and recession-related  
230 aridity index. These indices were chosen to incorporate time-varying climate and catchment  
231 conditions (TCCCs) in nonstationary modeling, of low-flow frequency and serving as candidate  
232 explanatory variables. The values of them at each year could be estimated from  
233 hydro-meteorological data. Annual precipitation ( $P$ ) and temperature ( $T$ ) are calculated directly  
234 by meteorological data. The remaining TCCCs indices need to be estimated indirectly. Detailed  
235 estimation procedures are shown as follows in following subsections. In addition to TCCCs  
236 indices, the three indices of human activity (irrigation area, population and gross domestic product)  
237 are included, and the reasons for selecting all indices are summarized in Table 2.

238 **2.3.1. Annual mean frequency of precipitation events ( $\lambda$ )**

239 Annual mean frequency of precipitation events is defined as an index to represent the  
240 intensity of precipitation recharge to the streamflow:

241

$$\lambda = \frac{1}{W} \sum_{w=1}^{w=W} \frac{N_w(A)}{t_r} \quad (6)$$

242 where  $N_w(A)$  is the number of daily rainfall events  $A$  (with values more than the threshold 0.5  
243 mm) in  $w^{th}$  windows with a length  $t_r$ ;  $W$  is the number of windows.

244 **2.3.2. Annual climate aridity index ( $AI_{ET}$ )**

245 The ratio of annual potential evaporation to precipitation, commonly known as the climate  
246 aridity index, has been used to assess the impacts of climate change on annual runoff (Arora, 2002;  
247 Jiang et al., 2015). The climate aridity index largely reflects the climatic regimes in a region and  
248 determines runoff rates (Arora, 2002). Therefore, we choose the annual climate aridity index as a  
249 measure of time-varying climate and catchment conditions and estimate its value in a whole region  
250 using

251 
$$AI_{ET} = \frac{ET}{P} \quad (7)$$

252 where  $P$  is annual areal precipitation (mm);  $ET$  is annual areal potential evapotranspiration.  
253 The Hargreaves equation (Hargreaves and Samani, 1985) is applied to calculate  $ET$  using the  
254 R-package ‘Evapotranspiration’ (Guo, 2014).

255 **2.3.3. Annual base-flow index ( $BFI$ )**

256 The base flow index ( $BFI$ ) is defined as the ratio of base flow to total flow. This index has  
257 been applied to quantify catchment conditions (e.g. soil, geology and storage-related descriptors)  
258 to explain hydrological drought severity (Van Loon and Laaha, 2015). We also choose annual base  
259 flow index ( $BFI$ ) as a measure of TCCCs.  $BFI$  is estimated using a hydrograph separation  
260 procedure in R-package ‘lfstat’ (Koffler and Laaha, 2013).

261    **2.3.4. Annual streamflow recession constant ( $K$ )**

262        Recession constant is an important catchment characteristic index measuring the time scale of  
263        the hydrological response and reflecting water retention ability in the upstream catchment (Botter  
264        et al., 2013). Various estimation methods have been developed to extract recession segments and to  
265        parameterize characteristic recession behavior of a catchment (Hall, 1968; Sawaske and Freyberg,  
266        2014; Tallaksen, 1995).

267        In this study, annual recession analysis (ARA) is performed to obtain annual streamflow  
268        recession constant ( $K$ ). In ARA, the linearized Deput-Boussinesq equation is used to parameterize  
269        characteristic recession behavior of a catchment and is written as

$$270 \quad -\frac{dQ_t}{dt} = \frac{1}{K} Q_t \quad (8)$$

271        where  $Q_t$  is the value at time  $t$ . Eq. (8) is investigated by plotting data points  $\frac{dQ_t}{dt}$  against  $Q_t$   
272        of all extracted recession segments from hydrographs at each year. The criteria of recession  
273        segments extraction [is-are](#) based on the Manual on Low-flow Estimation and Prediction (WMO,  
274        2009). Then, the annual recession rate ( $K^{-1}$ ) is estimated as the slope of fitted straight line of these  
275        data points with least square method. We calculated  $K$  using R-package 'lfstat' (Koffler and  
276        Laaha, 2013).

277    **2.3.5. Annual recession-related aridity index ( $AI_K$ )**

278        In this study, recession-related aridity index is defined as the ratio of recession rate ( $K^{-1}$ ) to

279 mean precipitation frequency ( $\lambda$ ), denoted as

280

$$AI_K = \frac{K^{-1}}{\lambda} \quad (9)$$

281 This ratio plays an important role in controlling ~~on~~-river flow regime (Botter et al., 2013;  
282 Gottschalk et al., 2013) and serves as an indicator measuring the recession-related aridity degree of  
283 the streamflow in river channel. For example, faster recession process or lower precipitation  
284 frequency may lead to increased runoff loss or decreased precipitation supply. Consequently, the  
285 higher the value  $AI_K$  is, the more likely low flow events occur, and vice versa.

286 **2.4 Parameter estimation**

287 The model parameters including  $\bar{\theta}_k (k=1,2,\dots,m)$  and  $\beta_{ik} (i=1,2,\dots,n, k=1,\dots,m)$  are  
288 estimated.  $\bar{\theta}_k (k=1,2,\dots,m)$  are estimated from outputs of stationary frequency analysis through  
289 maximum likelihood method. We have

290

$$L(\bar{\theta}_1, \bar{\theta}_2, \dots, \bar{\theta}_m) = \sum_{t=1}^{t=N} \ln \left[ f_Y(y_t | \bar{\theta}_1, \bar{\theta}_2, \dots, \bar{\theta}_m) \right] \quad (10)$$

291 where  $y_t$  is observed low flow at time  $t$ ;  $N$  is the number of samples. The parameters  $\bar{\theta}_k$   
292 ( $i=1,2,\dots,n, k=1,\dots,m$ ) are estimated through maximum likelihood method to produce  
293 nonstationary low-flow frequency curves:

294 
$$L \begin{pmatrix} \beta_{11}, \dots, \beta_{n1} \\ \dots \\ \beta_{1m}, \dots, \beta_{nm} \end{pmatrix} = \sum_{t=1}^{t=N} \ln \left\{ f_Y \left( y_t \left| \theta_1^t (z_1^t, \dots, z_n^t | \beta_{11}, \dots, \beta_{n1}), \dots, \theta_m^t (z_1^t, \dots, z_n^t | \beta_{1m}, \dots, \beta_{nm}) \right. \right) \right\} \quad (11)$$

295 The residuals (normalized randomized quintile residuals) are used to test the goodness-of-fit  
 296 of fitted model objects (Dunn and Symth, 1996):

297 
$$\hat{r}_t = \Phi^{-1} \left( F_Y \left( y_t \left| \hat{\theta}^t \right. \right) \right) \quad (12)$$

298 where  $F_Y(\cdot)$  is the cumulative distribution of  $y_t$ ;  $\Phi^{-1}(\cdot)$  is the inverse function of the standard  
 299 normal distribution. The distribution of the true residuals  $\hat{r}_t$  converges to standard normal if the  
 300 fitted model is correct. Worm plot (Buuren and Fredriks, 2001) is used to check whether  $\hat{r}_t$  have  
 301 a standard normal distribution.

302 **2.5 Model selection**

303 Model selection contains the selection of the type of probability distribution and the selection  
 304 of the explanatory variables to explain the response variables (i.e., distribution parameters  $\theta_1$  and  
 305  $\theta_2$ ). In order to obtain the final optimal model, the selection of the explanatory variables for  $\theta_1$   
 306 and  $\theta_2$  is conducted by a stepwise selection strategies (Stasinopoulos and Rigby, 2007; Venables,  
 307 2002): i.e. select a best subset of candidate explanatory variables for  $\theta_1$  using a forward approach  
 308 (which starts with no explanatory variable in the model and tests the addition of each explanatory  
 309 variable using a chosen model fit criterion); given this subset for  $\theta_1$  select another subset for  $\theta_2$   
 310 (forward). The stepwise selection strategies can get a series of stepwise models with different

311 numbers of explanatory variables, as shown in Fig1. In order to detect how the number of  
312 explanatory variables influences the performance of the model for describing non-stationarity, we  
313 investigate the five-eight types of stepwise models as shown in Table 3: the zero-covariate model  
314 or stationary model (M0), the time covariate model (M1), single physical covariate model M2  
315 (single TCCCs covariate model M2a or single HA covariate model M2b), the double physicaltwo  
316 TCCCs covariates model (M3)-and, the optimal number physicalTCCCs covariates model (M4),  
317 as shown in Table 2 the optimal HA covariates model (M5) and the final model (M6). The model  
318 fit criterion is based on the Akaike's information criterion (Akaike, 1974) as shown by the  
319 following

$$AIC = -2ML + 2df \quad (13)$$

321 where  $ML$  is the log-likelihood in Eq. (11) and  $df$  is the number of degrees of freedom. The  
322 model with the lower AIC value was considered better.

### 323 3. Study Area and Data

#### 324 3.1. The study area

325 The Weihe River, located in the southeast of the Northwest Loess Plateau, is the largest  
326 tributary of the Yellow River, China. The Weihe River has a drainage area of 134 766  $km^2$ ,  
327 covering the coordinates of 33°42'-37°20'N 104°18'-110°37'E (Fig. 42). This catchment  
328 generally has a semi-arid climate, with extensive sub-humid-continental monsoonal influence.

329 Average annual precipitation of the whole area over the period 1954-2009 is about 540 mm, and  
330 has a wide range (400-1000 mm) in various regions. Under the significant impacts of climate  
331 change and human activities in the Weihe River basin in recent decades, the hydrological regime  
332 of the river has changed over time (Du et al., 2015; Jiang et al., 2015; Xiong et al., 2015a).

333 | <Figure 42>

334 In the Weihe basin, the impacts of agricultural irrigation on runoff have been found to be  
335 significant (Jiang et al., 2015; Lin et al., 2012). Lin et al. (2012) mentioned that the annual runoff  
336 of the Weihe River was significantly affected by irrigation diversion of the Baoji Gorge irrigation  
337 area. The irrigated area of Baoji Gorge Irrigation Area increased over time since the founding of  
338 P.R. China in 1949, and due to one influential irrigation system project in that area, it became more  
339 than twice of the original one-irrigation area since 1971. Jiang et al. (2015) demonstrated that in  
340 the Weihe basin, irrigated area, as compared with the other indices e.g. population, gross domestic  
341 product and cultivated land area, was a more suitable human explanatory variable for explaining  
342 the time-varying behavior of annual runoff. Within the above background, it is important to  
343 considering the effects of human activities that mainly originate from irrigation diversion, and  
344 especially for studying low flow series in this basin. In this study, we use the available data  
345 (1980-2005) of the irrigation diversion system on plateau in Baoji Gorge Irrigation Area in Zhang  
346 (2008) to provide some information for the knowledge of low flow generation. The estimations of

347 annual recession rate ( $K^{-1}$ ) by the daily streamflow data are expected to incorporate the  
348 information of impacts of water diversions on the low flows in the river channel.

349 **3.2. Streamflow Data**

350 We used daily streamflow records (1954-2009) provided by the Hydrology Bureau of the  
351 Yellow River Conservancy Commission from both Huaxian station (with a drainage area of 106  
352 500 km<sup>2</sup>) and Xianyang station (with a drainage area of 46 480 km<sup>2</sup>). Low-flow extreme events  
353 were selected from the daily streamflow series using the widely-used annual minimum series  
354 method (WMO, 2009).  $AM_n$  is the annual minimum ~~n~~-day flow during hydrological year  
355 ~~defined to start beginning~~ on 1 March. Consequently,  $AM_1$ ,  $AM_7$ ,  $AM_{15}$  and  $AM_{30}$  are selected as  
356 low-flow extreme events in this study. The original measure unit of streamflow data (m<sup>3</sup>·s<sup>-1</sup>) is  
357 converted to 10<sup>-4</sup> m<sup>3</sup>·s<sup>-1</sup>·km<sup>-2</sup> ~~by dividing by the corresponding drainage area (km<sup>2</sup>)~~ for  
358 convenience of comparison of results between the Huaxian and Xianyang gauging stations

359 **3.3. Precipitation and temperature data**

360 We downloaded daily total precipitation and daily mean air temperature records for 19  
361 meteorological stations over the basin from the National Climate Center of the China  
362 Meteorological Administration (source: <http://cdc.cma.gov.cn>). The areal average daily series of  
363 both variables above Huaxian and Xianyang stations are calculated using the Thiessen polygon  
364 method (Szolgayova et al., 2014; Thiessen, 1911). The annual average temperature ( $T$ ) and annual

365 total precipitation ( $P$ ) over the period 1954-2009 are calculated for each catchment.

366 Human activity data (i.e. gross domestic product, population and irrigation area) were taken  
367 from annals of statistics provided by the Shaanxi Provincial Bureau of Statistics  
368 (<http://www.shaanxitj.gov.cn/>) and Gansu Provincial Bureau of Statistics (source:  
369 <http://www.gstj.gov.cn/>).

370

## 371 4. Results and discussion

### 372 4.1. Identification of nonstationarity

373 ~~Figure 2 shows that the Weihe River basin is characterized by a warm and humid summer~~  
374 ~~(June, July, and August) with low ratio of irrigated diversion, and by a cold and dry winter~~  
375 ~~(December, January, and February) with high ratio of irrigated diversion. The majority of the low~~  
376 ~~flow events in this basin occur in these two seasons and show a bimodal frequency distributions of~~  
377 ~~occurrence with two peaks in February and June, respectively (Fig. 2a). This result implies that the~~  
378 ~~generation of low flows may be influenced by more than one factor such as high ratio of irrigated~~  
379 ~~diversion, high air temperature or lack of precipitation.~~

380 <Figure 2>

381 Graphical representation and statistical test provide a preliminary analysis for low-flow  
382 nonstationarity. The graphical representations of time-series data help visualize the trends of

383 related variables (i.e. low-flow, TCCCs and HA variables), the density distributions of TCCCs  
384 variables and the correlations between low-flow variables and these explanatory variables. In Fig.  
385 3, ~~Overall~~overall, four annual minimum streamflow series ( $AM_1$ ,  $AM_7$ ,  $AM_{15}$  and  $AM_{30}$ ) in  
386 both Huaxian and Xianyang gauging stations show overall decreasing trends, as indicated by the  
387 fitted (dashed) trend lines ~~in Fig. 3~~. Compared with Huaxian, Xianyang has a larger runoff  
388 modulus (the flow per square kilometer) and a larger decrease in annual minimum streamflow  
389 series. For example, the decline slope of  $AM_{30}$  is  $-0.0725 (10^{-4} \text{ m}^3 \cdot \text{s}^{-1} \cdot \text{km}^{-2}/\text{yr})$  in Huaxian  
390 station ~~which while Xianyang station it is larger than~~  $-0.1338 (10^{-4} \text{ m}^3 \cdot \text{s}^{-1} \cdot \text{km}^{-2}/\text{yr})$  ~~in Xianyang~~  
391 station.

392 <Figure 3>

393 Figure 4 shows the kernel density estimations and time processes of ~~the eight candidate~~  
394 ~~explanatory~~TCCCs variables ~~(Sect. 2.3) reflecting the TCCCs~~ for both Huaxian (H) and Xianyang  
395 (X) stations. The results show that these variables have different variation patterns. For example,  
396 the mean frequency of precipitation events ( $\lambda$ ) has a decreasing trend, while temperature ( $T$ ) has  
397 an increasing trend. As presented by Fig. 5, three HA variables have a significant upward trend,  
398 especially the irrigation area IAR which is increased greatly after about 1970, suggesting that the  
399 impact of human activities in this basin has increased over time.

The significance of trends in the four annual minimum streamflow series and ~~eight~~

~~explanatory~~TCCCs variables is tested by the Mann-Kendall trend test (Kendall, 1975; Mann, 1945;

Yue et al., 2002), and the change —points in these series are detected by the Pettitt's test (Pettitt,

1979). The results in Table 3-4 show that in both Huaxian and Xianyang stations, the decreasing

trends in all the four low-flow series ( $AM_1$ ,  $AM_7$ ,  $AM_{15}$  and  $AM_{30}$ ) and two explanatory

variables ( $\lambda$  and  $P$ ), and the increasing trends in  $T$ ,  $ET$ , and  $AI_{ET}$  are significant at the 0.05

level (Table 34), but  $BFI$  shows no significant trends. However,  $K$  and  $AI_K$  had significantly

decreasing trends only in Huaxian station ( $p$ -value  $< 0.05$ ). The results of change-point detection

show that all low-flow series are located at 1968-1971 ( $p$ -value  $< 0.05$ ) except  $AM_{30}$  at

Xianyang station whose change point is located at 1993 ( $p$ -value  $< 0.05$ ); for the eight candidate

explanatory variables, the change points of the variables related to temperature ( $T$ ,  $ET$ ,  $AI_{ET}$ ) in

both stations are located at 1990-1993 ( $p$ -value  $< 0.05$ ), the change points of the variables related

to precipitation ( $\lambda$ ,  $P$ ) in both stations are close at 1984-1990 ( $p$ -value  $\leq 0.186$ ) and the change

points of the variables related to streamflow recession ( $K$ ,  $AI_K$ ) in Huaxian station are located at

1968-1971 ( $p$ -value  $< 0.05$ ). However,  $BFI$  in both stations and  $K$  and,  $AI_K$  in Xianyang

417 station show no significant change points.

418 A preliminary attribution analysis is performed using the Pearson correlation matrix to  
419 investigate the relations between the annual minimum series and eight candidate explanatory  
420 variables. Figure 65 indicates that there are significant linear correlations between the four  
421 minimum low-flow series ( $AM_1$ ,  $AM_7$ ,  $AM_{15}$  and  $AM_{30}$ ) and all the explanatory variables  
422 except GDP, with have the absolute values of Pearson correlation coefficients larger than 0.27  
423 ( $p$ -value  $< 0.05$ ). These potential physical causes of nonstationarity in low flows are further  
424 considered by establishing low-flow nonstationary model with TCCCs and HA variables in the  
425 following section.

426 <Figure 56>

## 427 4.2. Nonstationary frequency analysis models

### 428 4.2.1 Single covariate models

429 Figure 76 presents the AIC values of the three four types of models (M0, M1, M2a and  
430 M2bM2, M1 and M0) fitted for the low flow series ( $AM_1$ ,  $AM_7$ ,  $AM_{15}$  and  $AM_{30}$ ). Some  
431 interesting results are shown as follows. First, nonstationary models (M1, M2a and M2bM2 and  
432 M1) have lower AIC values than stationary model (M0), which suggests that nonstationary models  
433 are worth considering. Second, for Huaxian station, irrespective of the chosen explanatory

434 variables, the distribution type plays an important role in modeling nonstationary low flow series.

435 For example, PIII, GA and WEI distributions in  $AM_{15}$  ~~and~~  $AM_{30}$  ~~most~~ cases have lower AIC  
436 values than LOGNO and GEV distributions. However, for Xianyang, choosing a suitable  
437 explanatory variable may be more important than choosing a distribution type. For example,  
438 variables  $t$ ,  $P$ ,  $T$ , ~~and~~  $AI_{ET}$ , ~~POP~~ ~~and~~  $IAR$  in most cases have lower AIC values than the  
439 other explanatory variables. Finally, in Huaxian, ~~the lowest AIC values~~ ~~the best M2 models~~ for  
440 modeling  $AM_1$ ,  $AM_7$ ,  $AM_{15}$  and  $AM_{30}$  ~~are found in GEV M2b IAR, LOGNO M2b IAR,~~  
441 ~~PIII M2a AI<sub>K</sub> and GA M2a AI<sub>K</sub>, respectively~~ ~~are all found in the M2 AI<sub>K</sub> model (using AI<sub>K</sub>~~  
442 ~~as an explanatory variable)~~; while in Xianyang, ~~the lowest AIC values~~ ~~the best M2 models~~ for  
443 modeling  $AM_1$ ,  $AM_7$ ,  $AM_{15}$  and  $AM_{30}$  are ~~all~~ found in ~~the M2\_K, M2\_AI<sub>ET</sub>, M2\_AI<sub>ET</sub>~~  
444 ~~and M2\_T model~~ ~~GEV M2b IAR, GEV M2b IAR, PIII M2b IAR and GEV M2b IAR,~~  
445 respectively. These results indicated that ~~in~~ ~~for explaining nonstationarity of low flow in~~ ~~station, IAR is the most dominant HA variables, and AI<sub>K</sub> is the most dominant TCCCs variable~~  
446 ~~causing nonstationarity in AM<sub>1</sub>, AM<sub>7</sub>, AM<sub>15</sub> and AM<sub>30</sub>~~; while in Xianyang, the ~~most~~  
447 ~~dominant HA variables is IAR, the most dominant TCCCs variables~~ ~~causing nonstationarity in~~  
448 ~~AM<sub>1</sub>, AM<sub>7</sub>, AM<sub>15</sub> and AM<sub>30</sub> are K, AI<sub>ET</sub>, AI<sub>ET</sub> and T, respectively. Table 4~~  
449 ~~summarizes the above analysis.~~

451 <Figure 67>

452 Figure 87 shows the diagnostic assessment of the best M2 model the GA\_M2  
453 with the optimal explanatory variable) for  $AM_{30}$  in both Huaxian and Xianyang stations. The  
454 centile curves plots of GA\_M2 (Figs. 7a-8a and 7b-8b) show the observed values of  $AM_{30}$ , the  
455 estimated median and the areas between the 5th and 95th centiles. Figure 7a-8a shows the response  
456 relationship between  $AM_{30}$  and  $AI_K$  in Huaxian: the increase of  $AI_K$  means the smaller  
457 magnitude of low-flow events because a high value of  $AI_K$  (faster stream recession or fewer  
458 rainy days) may lead to faster water loss or less supply. In Fig. 7b-8b, the higher values of IAR T  
459 means the smaller magnitude of low flow events, which suggests that IAR T plays an important  
460 role in driving low-flow generation in Xianyang. Figs 7e-8c and 7d-8d show that the worm points  
461 are within the 95% confidence intervals, thereby indicating a good model fit and a reasonable  
462 model construction.

463 <Figure 78>

#### 464 4.2.2 Multiple covariate models

465 Figure 8-9 shows that the AIC values of stationary model (M0), time covariate model (M1),  
466 physical covariate models (M2a, M2b, M3, M4, M5 and M6) for  $AM_{30}$ . (M2, M3 and M4 with the  
467 corresponding optimal explanatory variables) for  $AM_1$ ,  $AM_7$ ,  $AM_{15}$  and  $AM_{30}$  in both  
468 Huaxian and Xianyang stations. As shown in Fig. 9, M4 (nonstationary GA distribution with the

域代码已更改

域代码已更改

469 optimal TCCCs variables) has a good performance; after adding the HA variables, M6 with the  
470 lowest AIC values is attained; it can be found that the combination of multiple TCCCs variables  
471 displays a-the major role in changing the low flows of Weihe River, but the influence of HA  
472 variables shouldn't be ignored. For all low flow series, the lowest AIC values are always found in  
473 the M4 models, suggesting that it is necessary to consider multiple explanatory variables for  
474 nonstationary modeling.

475 <Figure 89>

476 A summary of frequency analysis based on five types of models (M0, M1, M2, M3 and M4)  
477 for both Huaxian and Xianyang gauging stations nonstationary GA distribution  $AM_{30}$  is  
478 presented in Table 5 and Table 6, respectively. We choose to focus on M4, M5 and M6. When only  
479 using TCCCs variables to model nonstationary low-flow frequency distribution, the results of M4  
480 show the optimal combination of explanatory variables for all low-flow series contains more than  
481 three variables. For example, for  $AM_{30}$  of Huaxian, the optimal combination of TCCCs variables  
482 includes  $AI_K$ ,  $BFI$  and  $AI_{ET}$ . When only using HA variables, the results of M5 show  $IAR$  is  
483 important to the low flows in this area. And M4 has a better performance than M5. When using  
484 both TCCCs variables and HA variables, the results of M6 show the optimal combination contains  
485 multiple TCCCs variables and the irrigation area  $IAR$ . For Huaxian, the optimal combination of  
486 all explanatory variables is  $AI_K$ ,  $IAR$ ,  $BFI$  and  $P$ , while for Xianyang, the optimal

487 combination is IAR,  $AI_{ET}$  and BFI. For M4 and M3 models, the relative importance of  
488 selected explanatory variables is identified through the stepwise selection method. For instance,  
489 for  $AM_{30}$  in Xianyang (Table 5), temperature ( $T$ ) with highest relative importance, followed  
490 orderly by  $P$ , BFI and  $K$ . We can also find that if the candidatestwo TCCCs variables are  
491 highly correlated, they do not seem to be selected as the explanatory variables at the same time.  
492 For example, one of those variables in terms of only air temperature ( $T$ ), evapotranspiration ( $ET$ )  
493 and the climate aridity index ( $AI_{ET}$ ), only one of them will appear in the optimal combination-a  
494 best subset of eight candidates in the final optimum model. This suggests that multicollinearity  
495 problem in multiple variables analysis can be reduced, which will help obtain more reliable GLMs  
496 parameters for contribution analysis.

497 The diagnostic assessment of the best M4 model (GA\_M4)GA\_M6 model for  $AM_{30}$  at  
498 two stations is presented by Fig. 910. The centile curves plots of GA\_M46 (Figs. 910a and 910b)  
499 show the more sophisticated nonstationary modeling than GA\_M2 (Fig 78). When using GA\_M46  
500 to model  $AM_{30}$  in Huaxian (Fig. 9a), similar to GA\_M2, the lower low flows are found to also  
501 correspond to higher value of  $AI_K$ , but GA\_M46 are-is able to identify the more complex  
502 variation patterns of low flows through the incorporation of IAR, BFI and P. Figures 910c  
503 and 910d show that the data points of worm plots of GA\_M46 are almost within the 95%  
504 confidence intervals, thereby indicating an acceptable model fit and a reasonable model

505 construction.

506 <Figure 910>

507 Figure 40-11 presents the contribution of each selected explanatory variable to  
508  $\ln(\theta'_i) - \ln(\bar{\theta}_i)$  in observation year based on GA\_M46 for  $AM_{30}$  in Huaxian and Xianyang. We  
509 can find that for Huaxian, the simulation value of  $\ln(\theta'_i)$  frequently occur below  $\ln(\bar{\theta}_i)$  during  
510 the two periods of about 1970-1982 and 1993-2003, which is in accordance with the observed  
511 decrease in  $AM_{30}$  of Huaxian station during these periods. In the former period 1970-1982, ~~the~~  
512 ~~largest negative contribution is found in both  $AI_K$  and  $BFI$  contribute a lot of negative amount~~  
513 ~~to  $\ln(\theta'_i) - \ln(\bar{\theta}_i)$ , whereas during 1993-2003, the contribution of both  $AI_K$  and  $BFI$  becomes~~  
514 ~~much less. However,  $IAR$  has almost equal negative contribution to  $\ln(\theta'_i) - \ln(\bar{\theta}_i)$  in both~~  
515 ~~periods. Unlike the former ~~therethree~~ variables, the significant negative contribution of  $AI_{ET}$  is~~  
516 ~~only found in 1993-2003. For  $AM_{30}$  of Xianyang, the contribution of  $IAR$ ,  $AI_{ET}$  and  $BFI$  is~~  
517 ~~similar to that at Huaxian station in two periods, however  $AI_K$  is not included in the final model.~~  
518 ~~In the latter period 1993-2003, the largest negative contribution was found in  $AI_{ET}$ . These results~~  
519 ~~suggest that the significant change of  $AI_K$  (mainly because of faster streamflow recession after~~  
520 ~~nearly 1971) dominates the decrease in  $AM_{30}$  of Huaxian during 1970-1982, while after 1993,~~  
521 ~~the significant change of  $AI_{ET}$  (due to decreasing precipitation and increasing evapotranspiration)~~  
522 ~~has a main effect on the decrease in  $AM_{30}$  of Huaxian.~~

523

<Figure 11>524 **4.3. Discussion**

525 The impacts of both human activities and climate change on low flows of the study area ~~of~~  
526 ~~the Weihe basin~~ led to time-varying climate and catchment conditions (TCCCs). Nonstationary  
527 modeling for annual low flow series ~~considering using~~ TCCCs ~~variables and/or HA variables as~~  
528 ~~explanatory variables~~ is clearly different from either the stationary model (M0) or the time  
529 covariate model (M1). The result demonstrates that considering multiple drivers (e.g. the  
530 variability in catchment conditions), especially in such an artificially influenced river, is necessary  
531 for nonstationary modeling of annual low flow series.

532 In this study area, nonstationary modeling considering TCCCs is supported by the following  
533 facts and findings. For human activities, an important milestone representative is the completion  
534 and operation of the irrigation system on plateau in Baoji Gorge Irrigation Area since 1971 (Sect.  
535 3.1). Figure 5c shows the change of irrigation area in this basin. And ~~the~~ the change-point detection  
536 test in Sect. 4.1 shows that significant change points of both annual recession constant ( $K$ ) and  
537 low flow series occur exactly ~~in at~~ around 1971. This result demonstrates that changes in both  $K$   
538 and  $AM_{30}$  may involve a consequence of this project. In addition to human activities, climate  
539 change also makes a considerable contribution to nonstationarity of low flows, as suggested by  
540 nonstationary modeling using TCCCs variables with stepwise analysis. Actually, climate driving

541 pattern may strengthen after nearly 1990, which is indicated by change-point detection test of both  
542 annual mean temperature ( $T$ ) and annual precipitation ( $P$ ) as well as the behavior of annual low  
543 flow series after nearly 1990. Therefore, the temporal variability in irrigation area, streamflow  
544 recession, air temperature and precipitation (the frequency and volume of rain events) should be  
545 the main driving factors of generating low flow regimes in this basin. Overall, the causes of  
546 nonstationarity in category for two gauging stations have no clear difference, but have some  
547 differences in the relative importance. As shown in Table 5, when modeling the low-flow series of  
548 Huaxian using TCCCs variables, the optimal model (M4) preferred the variables are related to  
549 recession process; however, for Xianyang, the preferred variables isare related to temperature. The  
550 reason for this may be that as a downstream station, Huaxian station suffers more intensive human  
551 activity, so that the importance of temperature change to the low-flow change is reduced  
552 meanwhile the importance of streamflow recession (related to the capability of water storage)  
553 change is imprevenhanced.

554 Ignoring the negative impacts of the errors in estimating annual recession constant ( $K$ )  
555 which are caused by insufficient data points of extracted stream segments at some wet years may  
556 lead to the propagation of high errors in annual recession analysis, and accordingly affect the  
557 quality of nonstationary frequency analysis when using  $K$  as an explanatory variable. Further  
558 study will give more reliable estimation of  $K$  through improving annual recession analysis.

559        The related researches (Jiang et al., 2015; Yang and Yang, 2011; Yang and Yang, 2013; Zhang  
560        et al., 2015) have applied the Budyko framework to analyze the impacts of climate change and/or  
561        human activity on annual runoff. Indeed, for annual runoff, the Budyko framework is a better good  
562        method than the regression modeling method using in this study, because it used the mean annual  
563        water-energy balance equation to consider generation process of total runoff. Unfortunately, to our  
564        knowledge, there is a lack of the controls equation derived from basic physics laws for generation  
565        process of low flows. Therefore, we emphasize the importance of TCCCs variables to modeling of  
566        low-flow nonstationarity.

567        **5. Conclusion**

568        There is an increasing need to develop an effective nonstationary low-flow frequency model to  
569        deal with nonstationarities caused by climate change and time-varying anthropogenic activities. In  
570        this study, time-varying climate and catchment conditions (TCCCs) in the Weihe River basin were  
571        measured by annual time series of the eight indices, i.e., total precipitation ( $P$ ), mean frequency of  
572        precipitation events ( $\lambda$ ), temperature ( $T$ ), potential evapotranspiration ( $ET$ ), climate aridity index  
573        ( $AI_{ET}$ ), base-flow index ( $BFI$ ), recession constant ( $K$ ), and the recession-related aridity index ( $AI_K$ ).

574        The nonstationary distribution model was developed using both these eight TCCCs indices and/or  
575        there HA indices as candidate explanatory variables for frequency analysis of time-varying annual  
576        low flow series caused by multiple drivers. The main driving forces of the decrease in low flows in

577 the Weihe River include reduced precipitation, warming climate, increasing irrigation area and  
578 faster streamflow recession. Therefore, a complex deterioration mechanism resulting from these  
579 factors demonstrates that in this arid and semi-arid area, the water resources could be vulnerable to  
580 adverse environmental changes, thus portending increasing water shortages. The nonstationary  
581 low-flow model considering TCCCs can provide the knowledge of low-flow generation  
582 mechanism and give more reliable design of low flows for infrastructure and water supply.  
583

584 **Acknowledgements**

585 The study was financially supported by the National Natural Science Foundation of China  
586 (NSFC Grants 51525902 and 51479139), and projects from State Key Laboratory of Water  
587 Resources and Hydropower Engineering Science, Wuhan University. We greatly appreciate two  
588 reviewers for their insightful comments and constructive suggestions that helped us to improve the  
589 manuscript.

590

591 **Reference**

592 Akaike, H.: A new look at the statistical model identification, IEEE Transactions on  
593 Automatic Control, 19, 716-723, 1974.

594 Arora, V. K.: The use of the aridity index to assess climate change effect on annual runoff,  
595 Journal of Hydrology, 265, 164-177, 2002.

596 Botter, G., Basso, S., Rodriguez-Iturbe, I., and Rinaldo, A.: Resilience of river flow regimes,  
597 Proc Natl Acad Sci U S A, 110, 12925-12930, 2013.

598 Bradford, M. J. and Heinonen, J. S.: Low Flows, Instream Flow Needs and Fish Ecology in  
599 Small Streams, Canadian Water Resources Journal, 33, 165-180, 2008.

600 Buuren, S. V. and Fredriks, M.: Worm plot: a simple diagnostic device for modelling growth  
601 reference curves, Statistics in Medicine, 20, 1259-1277, 2001.

602 [Chen, X., Zhang, L., Xu, C.-Y., Zhang, J., and Ye, C.: Hydrological Design of Nonstationary](#)  
603 [Flood Extremes and Durations in Wujiang River, South China: Changing Properties, Causes, and](#)  
604 [Impacts, Mathematical Problems in Engineering, 2013,\(2013-6-2\), 2013, 211-244, 2013.](#)

605 [Cheng, L. and AghaKouchak, A.: Nonstationary precipitation Intensity-Duration-Frequency](#)  
606 [curves for infrastructure design in a changing climate, Sci Rep, 4, 7093, 2014.](#)

607 Dobson, A. J. and Barnett, A. G.: An Introduction to Generalized Linear Models, Third  
608 Edition, Journal of the Royal Statistical Society, 11, 272-272, 2012.

609 Du, T., Xiong, L., Xu, C.-Y., Gippel, C. J., Guo, S., and Liu, P.: Return period and risk  
610 analysis of nonstationary low-flow series under climate change, Journal of Hydrology, 527,  
611 234-250, 2015.

612 Dunn, P. K. and Symth, G. K.: Randomized quantile residuals, Journal of Computational and  
613 Graphical Statistics, 5, 236-244, 1996.

614 [Gilroy, K. L. and Mccuen, R. H.: A nonstationary flood frequency analysis method to adjust](#)  
615 [for future climate change and urbanization, Journal of Hydrology, s 414–415, 40-48, 2012.](#)

616 Giuntoli, I., Renard, B., Vidal, J. P., and Bard, A.: Low flows in France and their relationship  
617 to large-scale climate indices, Journal of Hydrology, 482, 105-118, 2013.

618 Gottschalk, L., Yu, K.-x., Leblois, E., and Xiong, L.: Statistics of low flow: Theoretical  
619 derivation of the distribution of minimum streamflow series, Journal of Hydrology, 481, 204-219,  
620 2013.

621 [Gu, X., Zhang, Q., Singh, V. P., Chen, X., and Liu, L.: Nonstationarity in the occurrence rate](#)  
622 [of floods in the Tarim River basin, China, and related impacts of climate indices, Global &](#)  
623 [Planetary Change, 142, 1-13, 2016.](#)

624 [Gu, X., Zhang, Q., Singh, V. P., and Shi, P.: Changes in magnitude and frequency of heavy](#)

625 [precipitation across China and its potential links to summer temperature, Journal of Hydrology, 547, 2017a.](#)

626 [Gu, X., Zhang, Q., Singh, V. P., and Shi, P.: Non - stationarities in the occurrence rate of heavy precipitation across China and its relationship to climate teleconnection patterns, International Journal of Climatology, 37, 4186-4198, 2017b.](#)

627 [Gu, X., Zhang, Q., Singh, V. P., and Shi, P.: Nonstationarity in timing of extreme precipitation across China and impact of tropical cyclones, Global & Planetary Change, 149, 153-165, 2017c.](#)

628 [Guo, D.: An R Package for Implementing Multiple Evapotranspiration Formulations, International Environmental Modelling and Software Society. 2014.](#)

629 [Hall, F. R.: Base flow recessions: A review, Water Resources Research, 4, 973-983, 1968.](#)

630 [Hargreaves, G. H. and Samani, Z. A.: Reference Crop Evapotranspiration From Temperature, 1, 96-99 1985.](#)

631 [Hewa, G. A., Wang, Q. J., McMahon, T. A., Nathan, R. J., and Peel, M. C.: Generalized extreme value distribution fitted by LH moments for low-flow frequency analysis, Water Resources Research, 43, 227-228-n/a n/a, 2007.](#)

632 [Jiang, C., Xiong, L., Guo, S., Xia, J., and Xu, C.-Y.: A process - based insight into nonstationarity of the probability distribution of annual runoff, Water Resources Research, 2017.](#)

633 [Jiang, C., Xiong, L., Wang, D., Liu, P., Guo, S., and Xu, C.-Y.: Separating the impacts of climate change and human activities on runoff using the Budyko-type equations with time-varying parameters, Journal of Hydrology, 522, 326-338, 2015.](#)

634 [Jiang, C., Xiong, L., Xu, C.-Y., and Guo, S.: Bivariate frequency analysis of nonstationary low - flow series based on the time - varying copula, Hydrological Processes, 29, 1521-1534, 2014 2015.](#)

635 [Jones, R. N., Chiew, F. H. S., Boughton, W. C., and Zhang, L.: Estimating the sensitivity of mean annual runoff to climate change using selected hydrological models, Advances in Water Resources, 29, 1419-1429, 2006.](#)

636 [Kam, J. and Sheffield, J.: Changes in the low flow regime over the eastern United States \(1962–2011\): variability, trends, and attributions, Climatic Change, 135, 639-653, 2015.](#)

637 [Kendall, M. G.: Rank Correlation Methods. , Griffin, London, 1975.](#)

638 [Koffler, D. and Laaha, G.: LFSTAT - Low-Flow Analysis in R, Egu General Assembly, 15, 2013.](#)

639 [Kormos, P. R., Luce, C. H., Wenger, S. J., and Berghuijs, W. R.: Trends and sensitivities of low streamflow extremes to discharge timing and magnitude in Pacific Northwest mountain streams, Water Resources Research, 52, 4990-5007, 2016.](#)

640 [Kwon, H.-H., Brown, C., and Lall, U.: Climate informed flood frequency analysis and](#)

660 prediction in Montana using hierarchical Bayesian modeling, *Geophysical Research Letters*, 35,  
661 | [L05404](#), 2008.

662 | López, J. and Francés, F.: Non-stationary flood frequency analysis in continental Spanish  
663 | rivers, using climate and reservoir indices as external covariates, *Hydrology and Earth System  
664 | Sciences*, 17, 3189-3203, 2013.

665 | Lin, Q. C., Huai-En, L. I., and Xi-Jun, W. U.: Impact of Water Diversion of Baojixia  
666 | Irrigation Area to the Weihe River Runoff, *Yellow River*, [2012](#), [34, 106-108](#), 2012.

667 | Liu, D., Guo, S., Lian, Y., Xiong, L., and Chen, X.: Climate-informed low-flow frequency  
668 | analysis using nonstationary modelling, *Hydrological Processes*, 29, 2112-2124, 2015.

669 | [Liu, J., Zhang, Q., Singh, V. P., and Shi, P.: Contribution of multiple climatic variables and  
670 | human activities to streamflow changes across China, \*Journal of Hydrology\*, 545, 145-162 2017.](#)

671 | Mann, H. B.: Nonparametric Tests Against Trend, *Econometrica*, 13, 245-259, 1945.

672 | Matalas, N. C.: Probability distribution of low flows, U.S. Geological Survey professional  
673 | Paper, 434-A, 1963.

674 | Milly, P. C. D., Betancourt, J., Falkenmark, M., Hirsch, R. M., Kundzewicz, Z. W.,  
675 | Lettenmaier, D. P., and Stouffer, R. J.: Stationarity Is Dead: Whither Water Management?, *Science*,  
676 | 319, 573-574, 2008.

677 | [Mondal, A. and Mujumdar, P. P.: Modeling non-stationarity in intensity, duration and  
678 | frequency of extreme rainfall over India, \*Journal of Hydrology\*, 521, 217-231, 2015.](#)

679 | Pettitt, A. N.: A Non-Parametric Approach to the Change-Point Problem, *Journal of the Royal  
680 | Statistical Society*, 28, [126-135](#), 1979.

681 | Richard, W. K., Marc, B. P., and Philippe, N.: Statistics of extremes in hydrology, *Advances  
682 | in Water Resources*, 25, 1287-1304, 2002.

683 | Rigby, R. A. and Stasinopoulos, D. M.: Generalized additive models for location, scale and  
684 | shape, *Appl. Statist.*, 54, 507-554, 2005.

685 | Roderick, M. L., Sun, F., Lim, W. H., and Farquhar, G. D.: A general framework for  
686 | understanding the response of the water cycle to global warming over land and ocean, *Hydrology  
687 | & Earth System Sciences Discussions*, 10, 15263-15294, 2013.

688 | Sadri, S., Kam, J., and Sheffield, J.: Nonstationarity of low flows and their timing in the  
689 | eastern United States, *Hydrology & Earth System Sciences Discussions*, 12, 2761-2798, 2015.

690 | Salas, J. D.: Analysis and modeling of hydrologic time series, *Handbook of Hydrology*, 1993.

691 | Sawaske, S. R. and Freyberg, D. L.: An analysis of trends in baseflow recession and  
692 | low-flows in rain-dominated coastal streams of the pacific coast, *Journal of Hydrology*, 519,  
693 | 599-610, 2014.

694 | Smakhtin, V. U.: Low flow hydrology: a review, *Journal of Hydrology*, [240, 147-186](#), 2001.

695 Stasinopoulos, D. M. and Rigby, R. A.: Generalized additive models for location scale and  
696 shape (GAMLSS) in R, *Journal of Statistical Software*, 23, 2007.

697 Strupczewski, W. G., Singh, V. P., and Feluch, W.: Non-stationary approach to at-site flood  
698 frequency modeling I. Maximum likelihood estimation, *Journal of Hydrology*, 248, 123-142, 2001.

699 Szolgayova, E., Parajka, J., Blöschl, G., and Bucher, C.: Long term variability of the Danube  
700 River flow and its relation to precipitation and air temperature, *Journal of Hydrology*, 519,  
701 871-880, 2014.

702 Tallaksen, L. M.: A review of baseflow recession analysis, *Journal of Hydrology*, 165,  
703 349-370, 1995.

704 Tallaksen, L. M., Madsen, H., and Hisdal, H.: *Hydrological Drought- Processes and  
705 Estimation Methods for Streamflow and Groundwater*, Elsevier B.V., the Netherlands, 2004.

706 [Tang, Y., Xi, S., Chen, X., and Lian, Y.: Quantification of Multiple Climate Change and  
707 Human Activity Impact Factors on Flood Regimes in the Pearl River Delta of China, Advances in  
708 Meteorology, 2016, 1-11, 2015.](#)

709 Thiessen, A. H.: Precipitation averages for large areas, *Monthly Weather Review*, 39,  
710 1082-1084, 1911.

711 Van Loon, A. F. and Laaha, G.: Hydrological drought severity explained by climate and  
712 catchment characteristics, *Journal of Hydrology*, 526, 3-14, 2015.

713 Venables, W. N. a. R., B. D. (2002) *Modern Applied Statistics with S*. Fourth edition, 2002.

714 Villarini, G., Smith, J. A., and Napolitano, F.: Nonstationary modeling of a long record of  
715 rainfall and temperature over Rome, *Advances in Water Resources*, 33, 1256-1267, 2010.

716 Villarini, G., Smith, J. A., Serinaldi, F., Bales, J., Bates, P. D., and Krajewski, W. F.: Flood  
717 frequency analysis for nonstationary annual peak records in an urban drainage basin, *Advances in  
718 Water Resources*, 32, 1255-1266, 2009.

719 Villarini, G. and Strong, A.: Roles of climate and agricultural practices in discharge changes  
720 in an agricultural watershed in Iowa, *Agriculture, Ecosystems & Environment*, 188, 204-211,  
721 2014.

722 WMO: *Manual on Low-flow Estimation and Prediction*. WMO-No.1029, Switzerland, 2009.

723 Xiong, L., Du, T., Xu, C.-Y., Guo, S., Jiang, C., and Gippel, C. J.: Non-Stationary Annual  
724 Maximum Flood Frequency Analysis Using the Norming Constants Method to Consider  
725 Non-Stationarity in the Annual Daily Flow Series, *Water Resources Management*, 29, 3615-3633,  
726 2015

727 [Xiong, L., Jiang, C., and Du, T.: Statistical attribution analysis of the nonstationarity of the  
728 annual runoff series of the Weihe River, Water Science & Technology, 70, 939-946, 2014.](#)

729 [Yan, L., Xiong, L., Liu, D., Hu, T., and Xu, C.-Y.: Frequency analysis of nonstationary](#)

730 annual maximum flood series using the time - varying two - component mixture distributions,  
731 Hydrological Processes, 31, 69–89, 2017.

732 Yang, H. and Yang, D.: Derivation of climate elasticity of runoff to assess the effects of  
733 climate change on annual runoff, Water Resources Research, 47, 197-203, 2011.

734 Yang, H. and Yang, D.: Evaluating attribution of annual runoff change: according to climate  
735 elasticity derived using Budyko hypothesis, Egu General Assembly, 15, 14029, 2013.

736 Yu, K.-x., Xiong, L., and Gottschalk, L.: Derivation of low flow distribution functions using  
737 copulas, Journal of Hydrology, 508, 273-288, 2014.

738 Yue, S., Pilon, P., and Cavadias, G.: Power of the Mann–Kendall and Spearman's rho tests for  
739 detecting monotonic trends in hydrological series, Journal of Hydrology, 259, 254-271, 2002.

740 Zhang, Q., Gu, X., Singh, V. P., and Xiao, M.: Flood frequency analysis with consideration of  
741 hydrological alterations: Changing properties, causes and implications, Journal of Hydrology, 519,  
742 803-813, 2014.

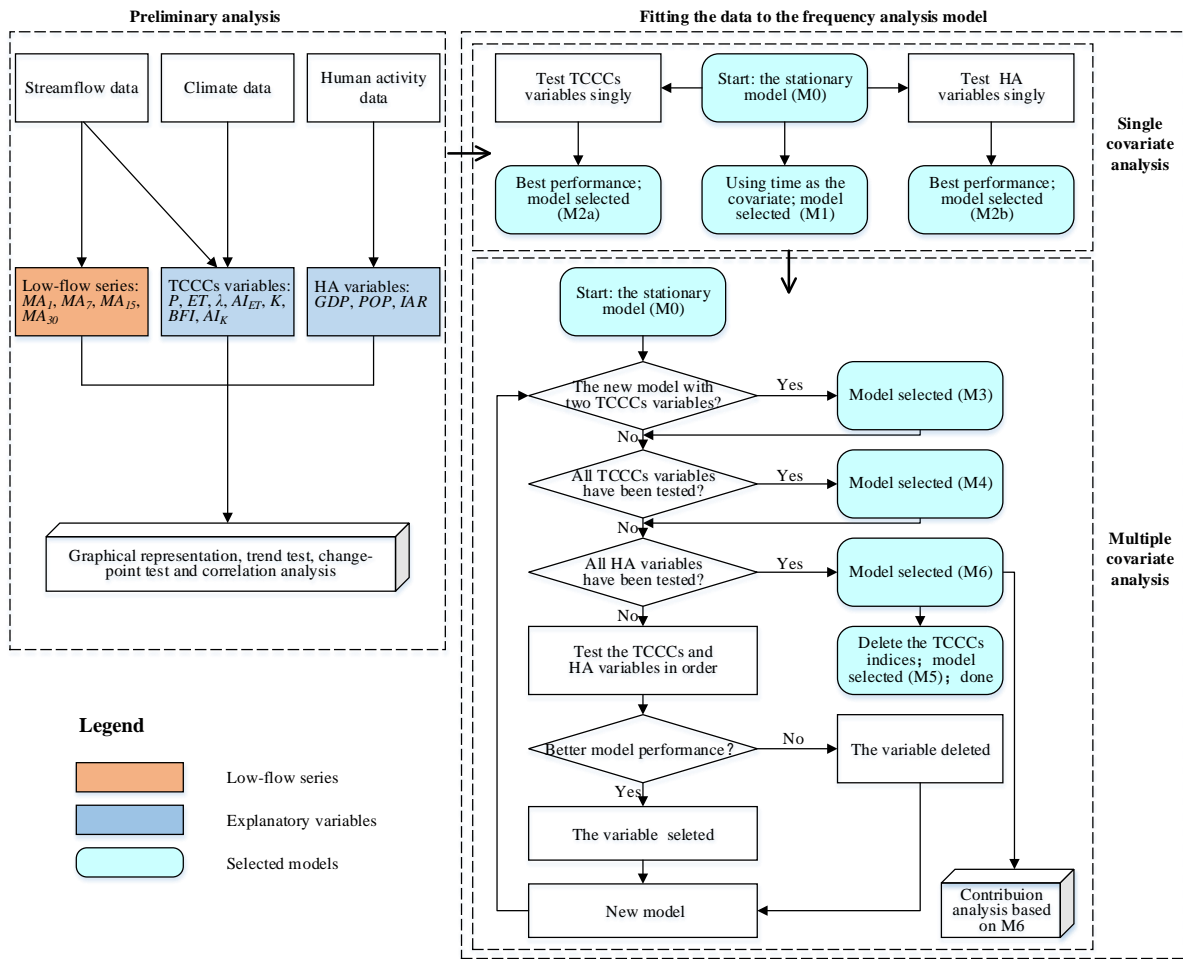
743 Zhang, Q., Gu, X., Singh, V. P., Xiao, M., and Chen, X.: Evaluation of flood frequency under  
744 non-stationarity resulting from climate indices and reservoir indices in the East River basin, China,  
745 Journal of Hydrology, 527, 565-575, 2015.

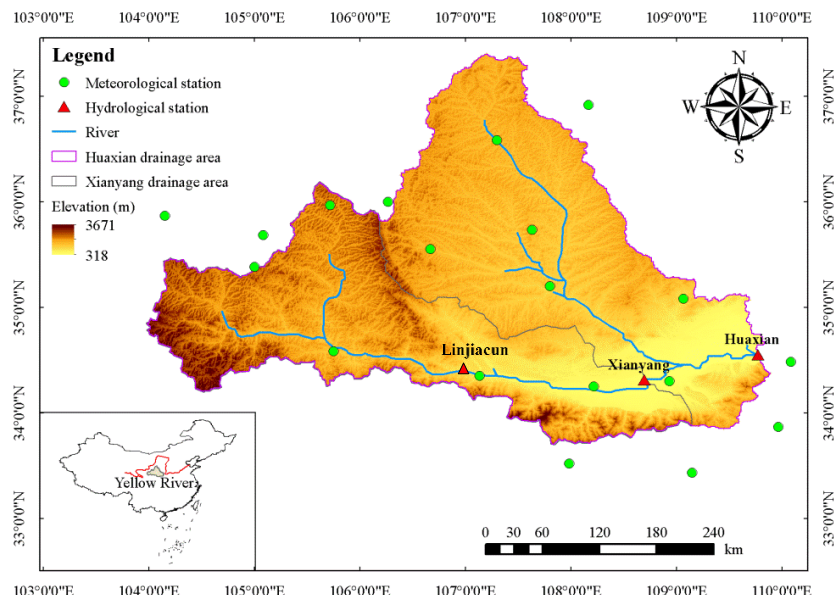
746 Zhang, S., Yang, H., Yang, D., and Jayawardena, A. W.: Quantifying the effect of vegetation  
747 change on the regional water balance within the Budyko framework, Geophysical Research Letters,  
748 43, 1140-1148, 2015.

749 Zhang, Y. P.: Economical water-use mode research of Baoji Gorge Irrigation Area based on  
750 WebGIS. Chinese, 2008.

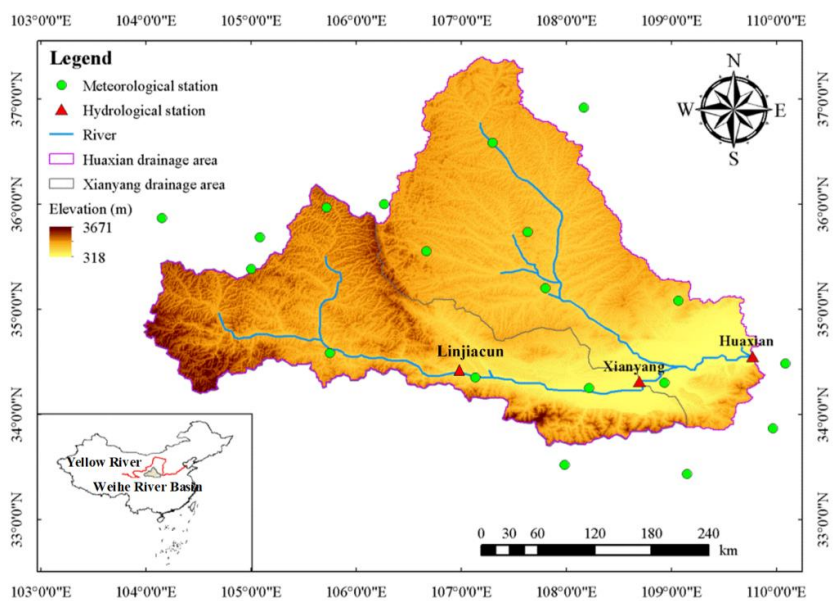
751

752

754 **Figure**757 **Figure 1. The framework of nonstationary low-flow frequency analysis.**



759



760

761 | Figure 42. Location, topography, hydro-meteorological stations and river systems of the Weihe

762 River basin.

763

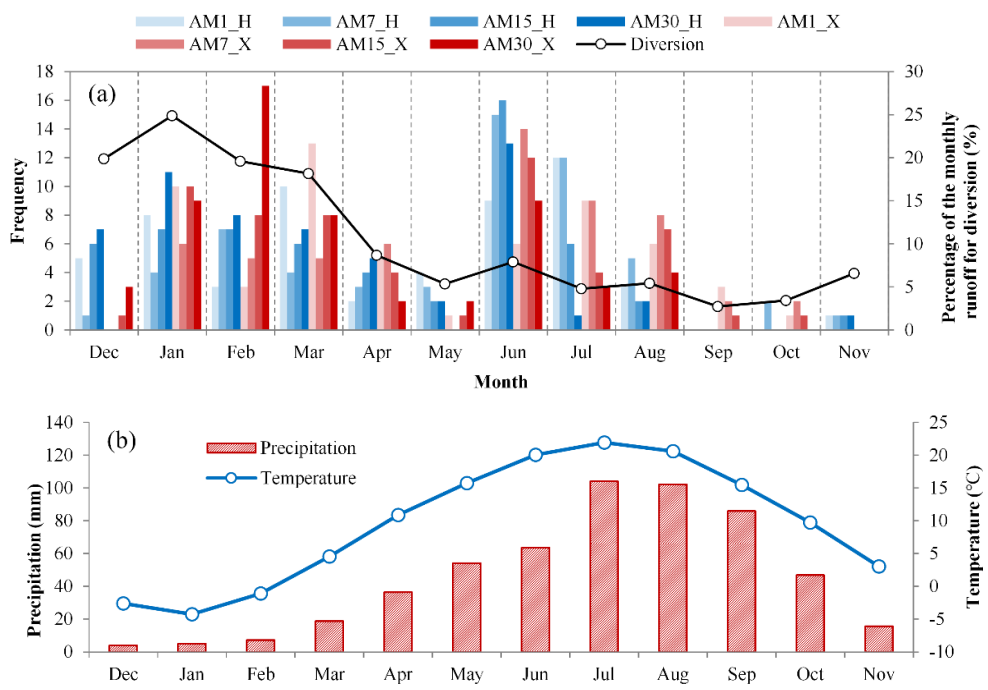
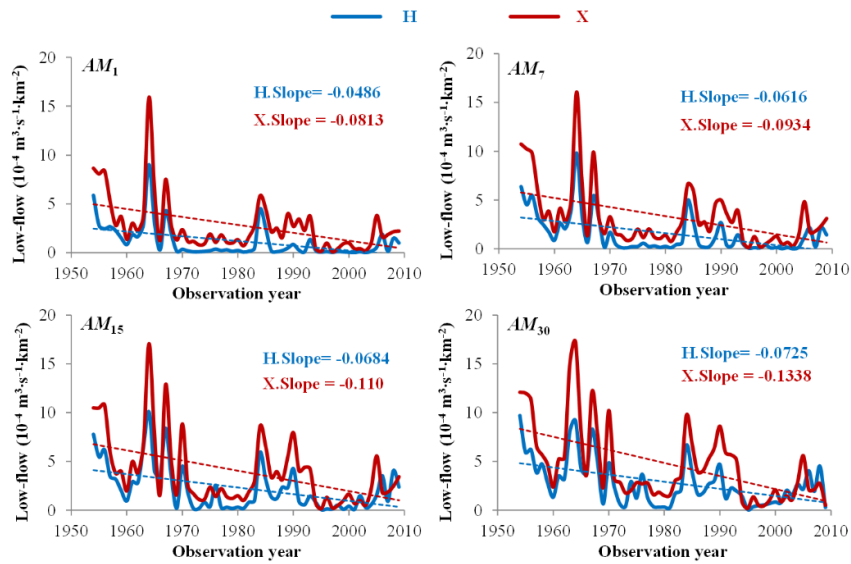
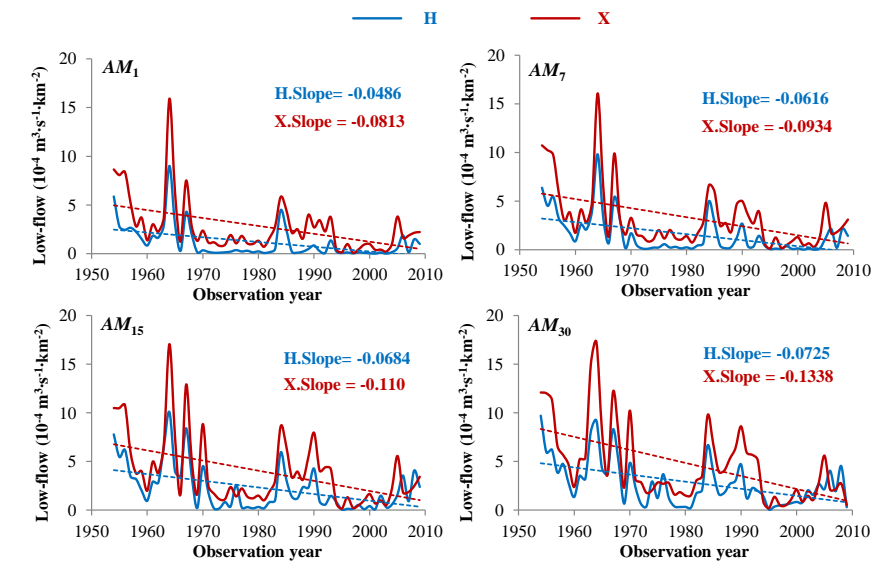


Figure 2. Overview of annual low flows and important environment factors using mean monthly data. (a) is frequency distributions of the occurrence time of the annual minimum flows with four durations at Huaxian (H) and Xianyang (X); the black line is mean monthly diversion (1980 to 2005) in Baoji Gorge area. (b) Mean monthly precipitation and temperature from 1954 to 2009.



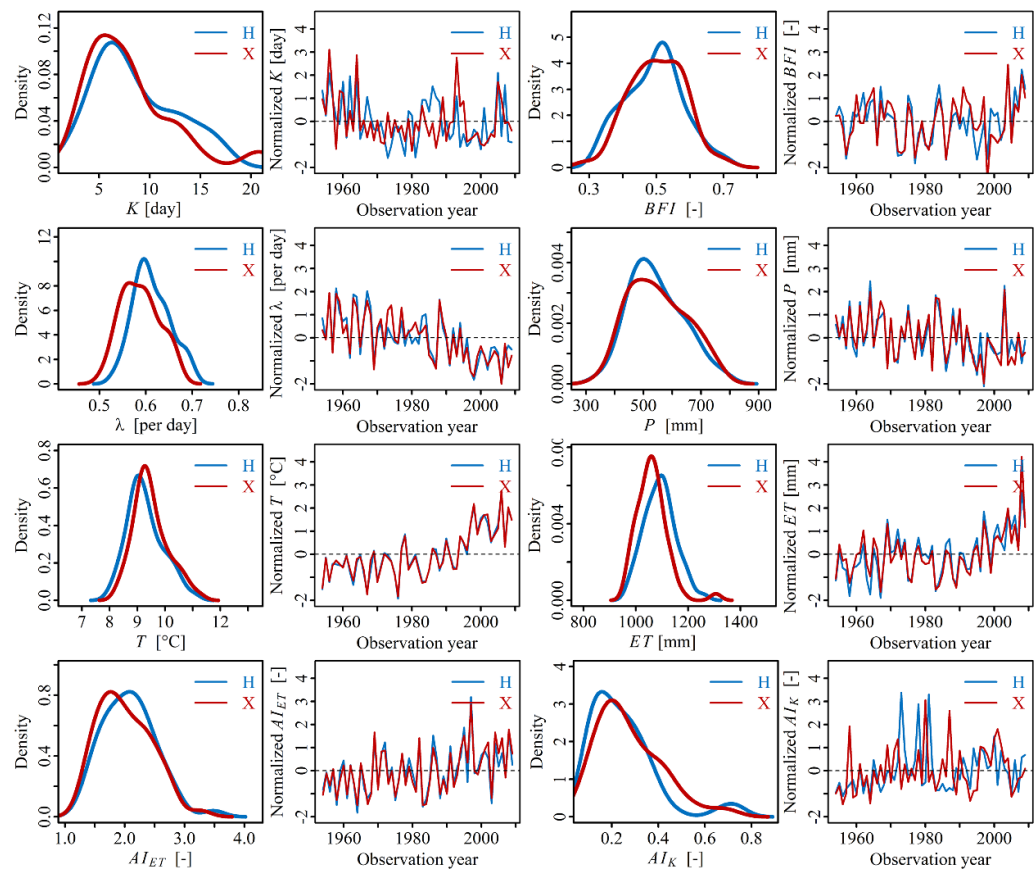
771

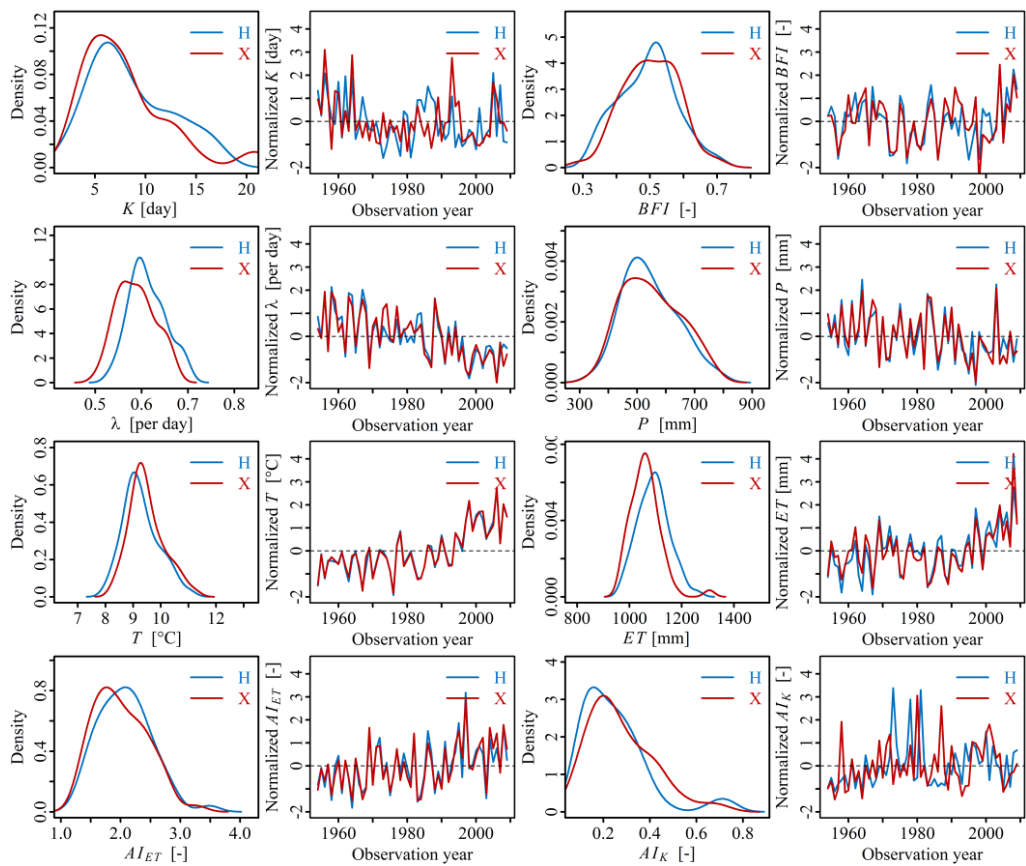


772

773 Figure 3. The annual minimum low flows and fitted trend lines in both Huaxian (H) and Xianyang  
 774 (X) gauging stations.

775

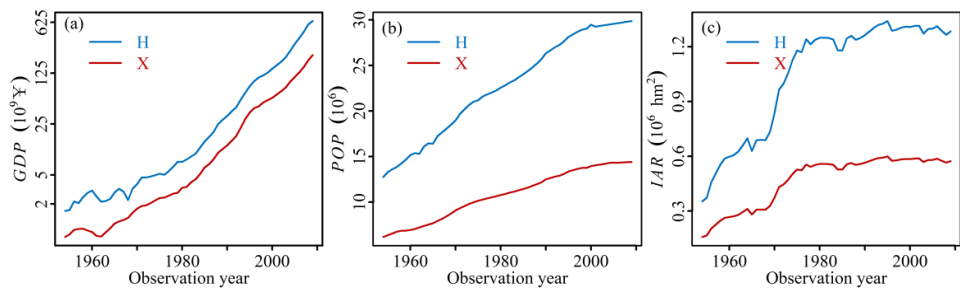




777

778 Figure 4. Frequency distributions (using the kernel density estimations) and ~~annual series of eight~~  
 779 ~~candidate explanatory variables~~ ~~time series processes of TCCCs variables~~ in both Huaxian (H) and  
 780 Xianyang (X) stations.

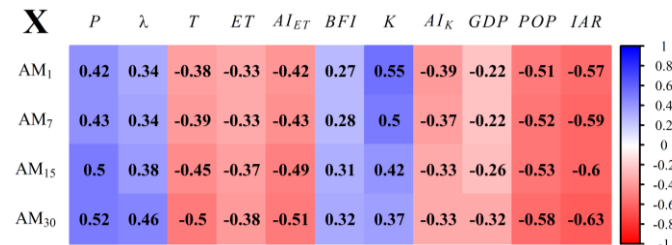
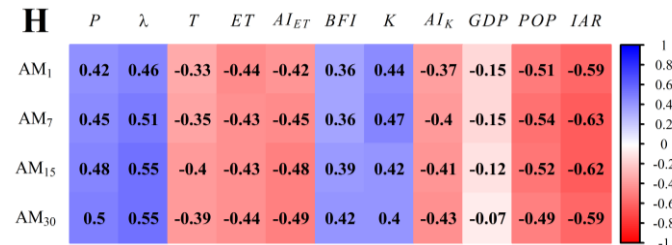
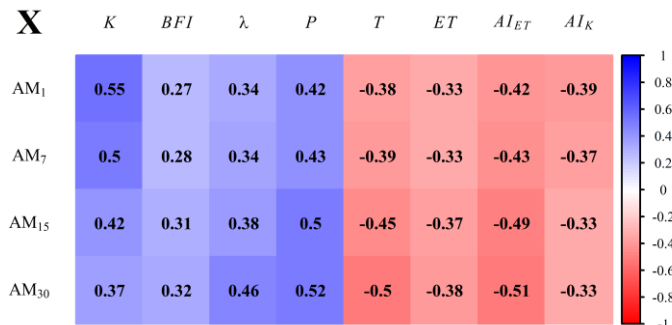
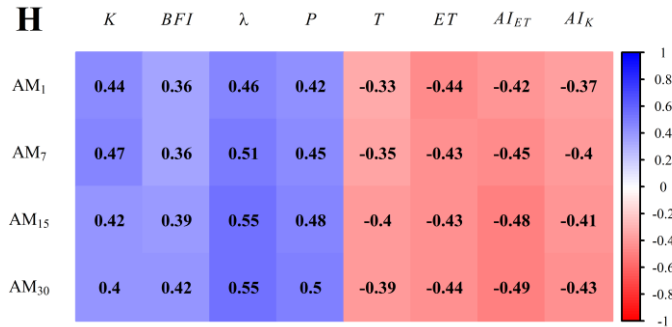
781



782

783 Figure 5. HA indices in both Huaxian (H) and Xianyang (X). (a), (b) and (c) are for population  
 784 (POP), gross domestic production (GDP) and irrigated area (IAR), respectively.

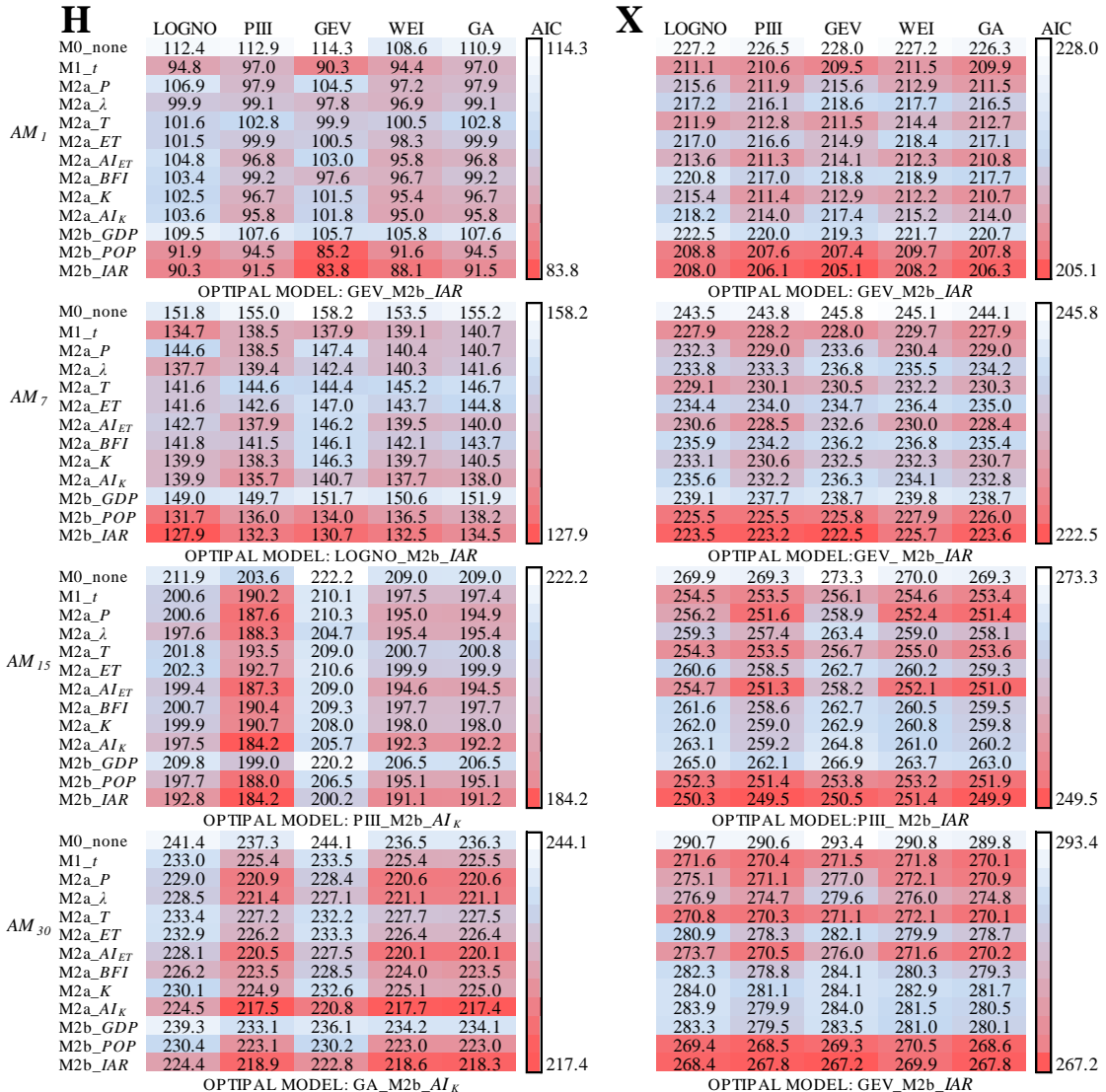
785



788 | Figure 56. The Pearson correlation coefficients matrix between the annual minimum flow series  
789 | and ~~eight~~ candidate explanatory variables in Huaxian (H) and Xianyang (X) stations; the darker  
790 | color intensity represents a higher level of correlation (blue indicates positive correlation, and red  
791 | indicates negative correlations).

792 |

<b>H</b>	LOGNO	PIII	GEV	WEI	GA	AIC	<b>X</b>	LOGNO	PIII	GEV	WEI	GA	AIC
<i>AM<sub>1</sub></i>	M0_none	112.4	112.9	114.3	108.6	110.9		227.2	226.5	228.0	227.2	226.3	228.0
	M1_t	94.8	97.0	90.3	94.4	97.0		211.1	210.6	209.5	211.5	209.9	
	M2_K	102.5	96.7	101.5	95.4	96.7		215.4	211.4	212.9	212.2	210.7	
	M2_BFI	103.4	99.2	97.6	96.7	99.2		220.8	217.0	218.8	218.9	217.7	
	M2_λ	99.9	99.1	97.8	96.9	99.1		217.2	216.1	218.6	217.7	216.5	
	M2_P	106.9	97.9	104.5	97.2	97.9		215.6	211.9	215.6	212.9	211.5	
	M2_T	101.6	102.8	99.9	100.5	102.8		211.9	212.8	211.5	214.4	212.7	
	M2_ET	101.5	99.9	100.5	98.3	99.9		217.0	216.6	214.9	218.4	217.1	
	M2_AI <sub>ET</sub>	104.8	96.8	103.0	95.8	96.8		213.6	211.3	214.1	212.3	210.8	
	M2_AI <sub>K</sub>	103.6	95.8	101.8	95.0	95.8	90.3	218.2	214.0	217.4	215.2	214.0	209.5
OPTIPAL MODEL: AIC(GEV, <i>t</i> )= 90.3													
<i>AM<sub>7</sub></i>	M0_none	151.8	155.0	158.2	153.5	155.2		243.5	243.8	245.8	245.1	244.1	245.8
	M1_t	134.7	138.5	137.9	139.1	140.7		227.9	228.2	228.0	229.7	227.9	
	M2_K	139.9	138.3	146.3	139.7	140.5		233.1	230.6	232.5	232.3	230.7	
	M2_BFI	141.8	141.5	146.1	142.1	143.7		235.9	234.2	236.2	236.8	235.4	
	M2_λ	137.7	139.4	142.4	140.3	141.6		233.8	233.3	236.8	235.5	234.2	
	M2_P	144.6	138.5	147.4	140.4	140.7		232.3	229.0	233.6	230.4	229.0	
	M2_T	141.6	144.6	144.4	145.2	146.7		229.1	230.1	230.5	232.2	230.3	
	M2_ET	141.6	142.6	147.0	143.7	144.8		234.4	234.0	234.7	236.4	235.0	
	M2_AI <sub>ET</sub>	142.7	137.9	146.2	139.5	140.0		230.6	228.5	232.6	230.0	228.4	
	M2_AI <sub>K</sub>	139.9	135.7	140.7	137.7	138.0	134.7	235.6	232.2	236.3	234.1	232.8	227.9
OPTIPAL MODEL: AIC(PIII, <i>t</i> )= 134.7													
<i>AM<sub>15</sub></i>	M0_none	211.9	203.6	222.2	209.0	209.0		269.9	269.3	273.3	270.0	269.3	273.3
	M1_t	200.6	190.2	210.1	197.5	197.4		254.5	253.5	256.1	254.6	253.4	
	M2_K	199.9	190.7	208.0	198.0	198.0		262.0	259.0	262.9	260.8	259.8	
	M2_BFI	200.7	190.4	209.3	197.7	197.7		261.6	258.6	262.7	260.5	259.5	
	M2_λ	197.6	188.3	204.7	195.4	195.4		259.3	257.4	263.4	259.0	258.1	
	M2_P	200.6	187.6	210.3	195.0	194.9		256.2	251.6	258.9	252.4	251.4	
	M2_T	201.8	193.5	209.0	200.7	200.8		254.3	253.5	256.7	255.0	253.6	
	M2_ET	202.3	192.7	210.6	199.9	199.9		260.6	258.5	262.7	260.2	259.3	
	M2_AI <sub>ET</sub>	199.4	187.3	209.0	194.6	194.5		254.7	251.3	258.2	252.1	251.0	
	M2_AI <sub>K</sub>	197.5	184.2	205.7	192.3	192.2	184.2	263.1	259.2	264.8	261.0	260.2	251.0
OPTIPAL MODEL: AIC(PIII, <i>AI<sub>K</sub></i> )= 184.2													
<i>AM<sub>30</sub></i>	M0_none	241.4	237.3	244.1	236.5	236.3		290.7	290.6	293.4	290.8	289.8	293.4
	M1_t	233.0	225.4	233.5	225.4	225.5		271.6	270.4	271.5	271.8	270.1	
	M2_K	230.1	224.9	232.6	225.1	225.0		284.0	281.1	284.1	282.9	281.7	
	M2_BFI	226.2	223.5	228.5	224.0	223.5		282.3	278.8	284.1	280.3	279.3	
	M2_λ	228.5	221.4	227.1	221.1	221.1		276.9	274.7	279.6	276.0	274.8	
	M2_P	229.0	220.9	228.4	220.6	220.6		275.1	271.1	277.0	272.1	270.9	
	M2_T	233.4	227.2	232.2	227.7	227.5		270.8	270.3	271.1	272.1	270.1	
	M2_ET	232.9	226.2	233.3	226.4	226.4		280.9	278.3	282.1	279.9	278.7	
	M2_AI <sub>ET</sub>	228.1	220.5	227.5	220.1	220.1		273.7	270.5	276.0	271.6	270.2	
	M2_AI <sub>K</sub>	224.5	217.5	220.8	217.7	217.4	217.4	283.9	279.9	284.0	281.5	280.5	270.1
OPTIPAL MODEL: AIC(GA, <i>AI<sub>K</sub></i> )= 217.4													
OPTIPAL MODEL: AIC(GA, <i>T</i> )= 270.1													



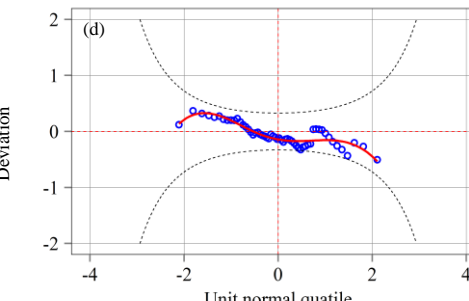
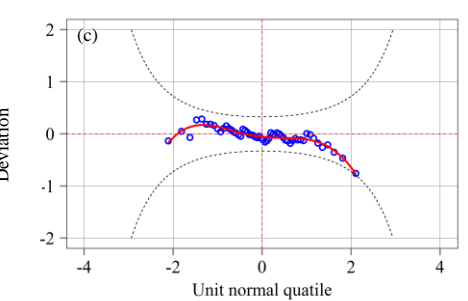
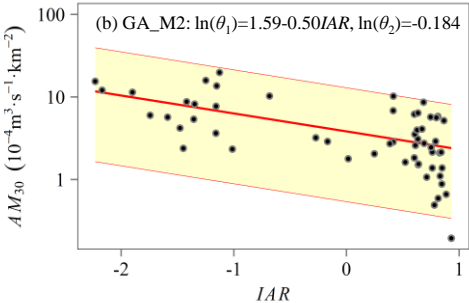
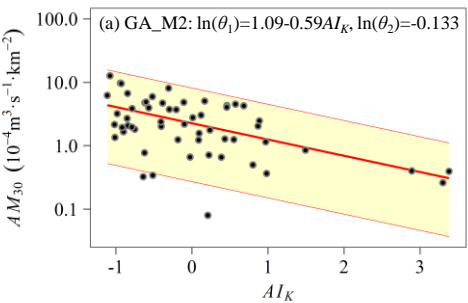
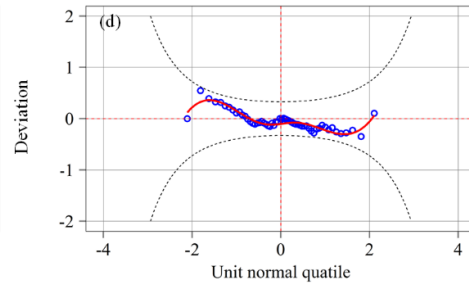
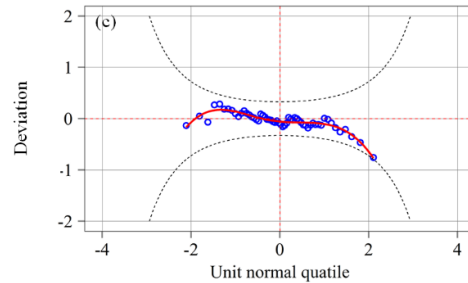
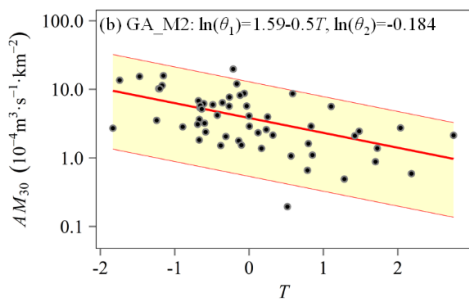
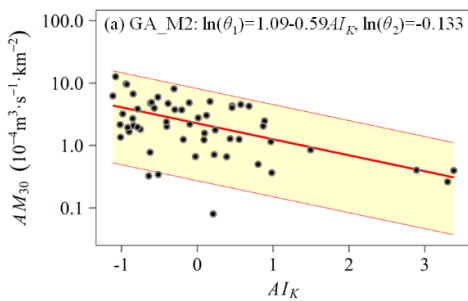
794

795 Figure 67. Comparisons among M0, M1 and M2 based on the AIC values for the four observed

796 low-flow series in Huaxian (H) at left panel and Xianyang (X) at right panel; darker red color

797 represents a higher goodness of fit.

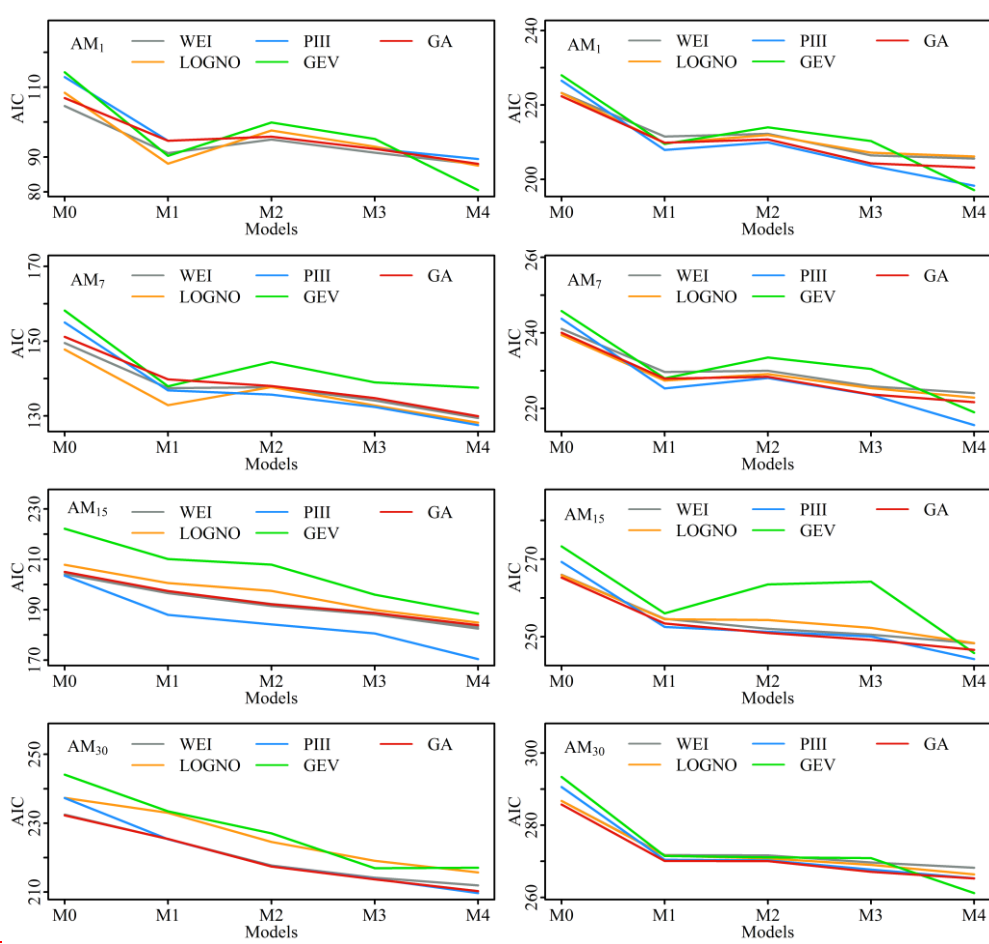
798

**H**

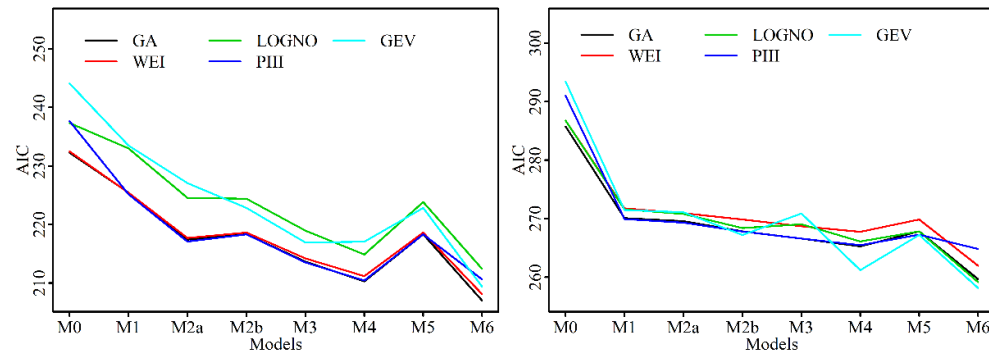
803     Figure 78. Performance assessments of ~~the best M2 model (GA\_M2)~~ GA\_M2 for  $AM_{30}$  in  
804     Huaxian (H) at left panel and Xianyang (X) at right panel. (a) and (b) are the centile curves plots  
805     of GA\_M2 (red lines represent the centile curves estimated by GA\_M2; the 50th centile curves are  
806     indicated by thick red; the yellow-filled areas are between the 5th and 95th centile curves; the  
807     black points indicate the observed series); (c) and (d) are the worm plots of GA\_M2 for the  
808     goodness-of-fit test; a reasonable model fit should have the data points fall within the 95%  
809     confidence intervals (between the two red dashed curves).

**H****X**

810



811

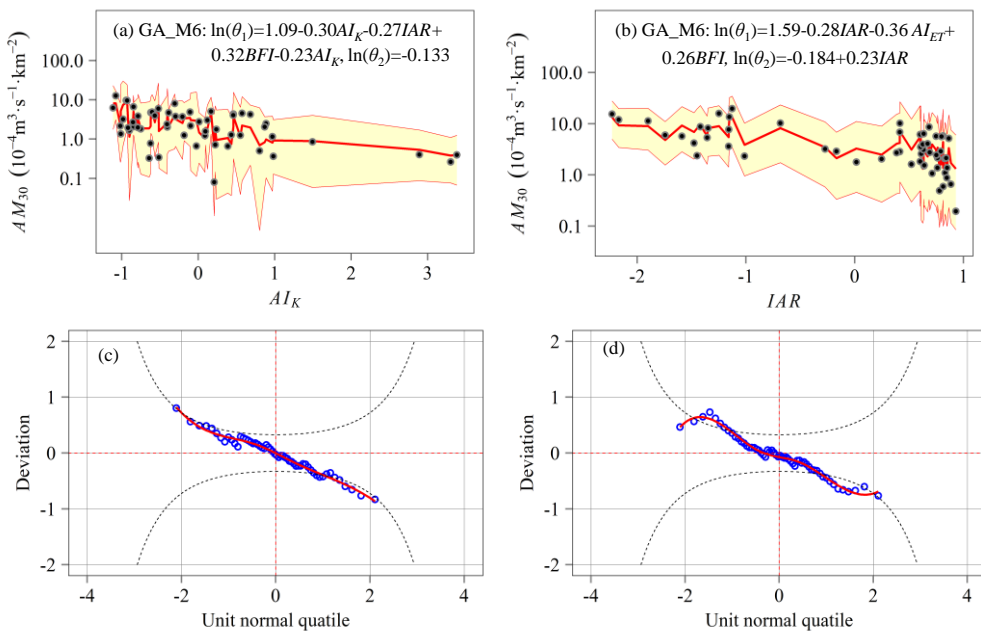
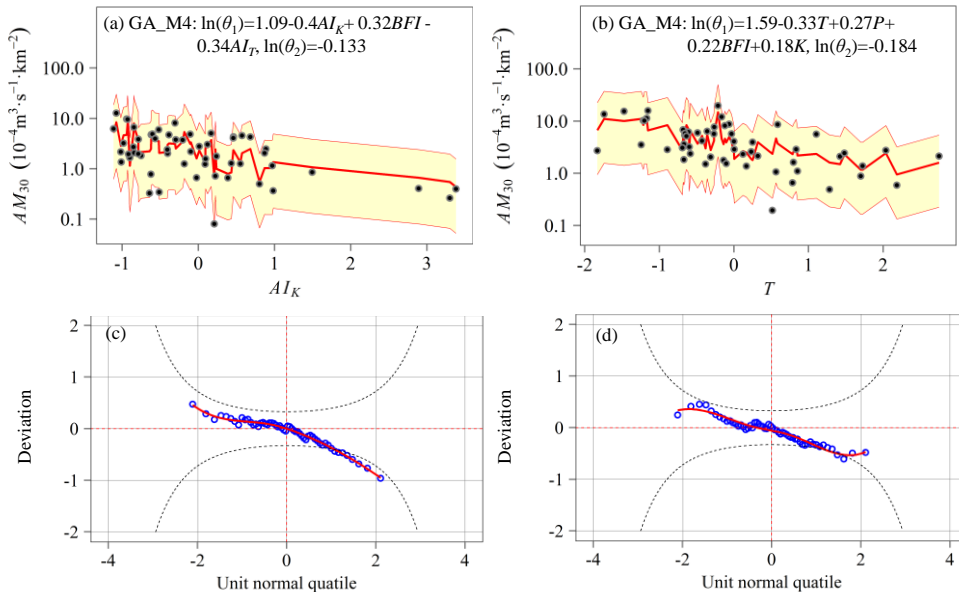


812

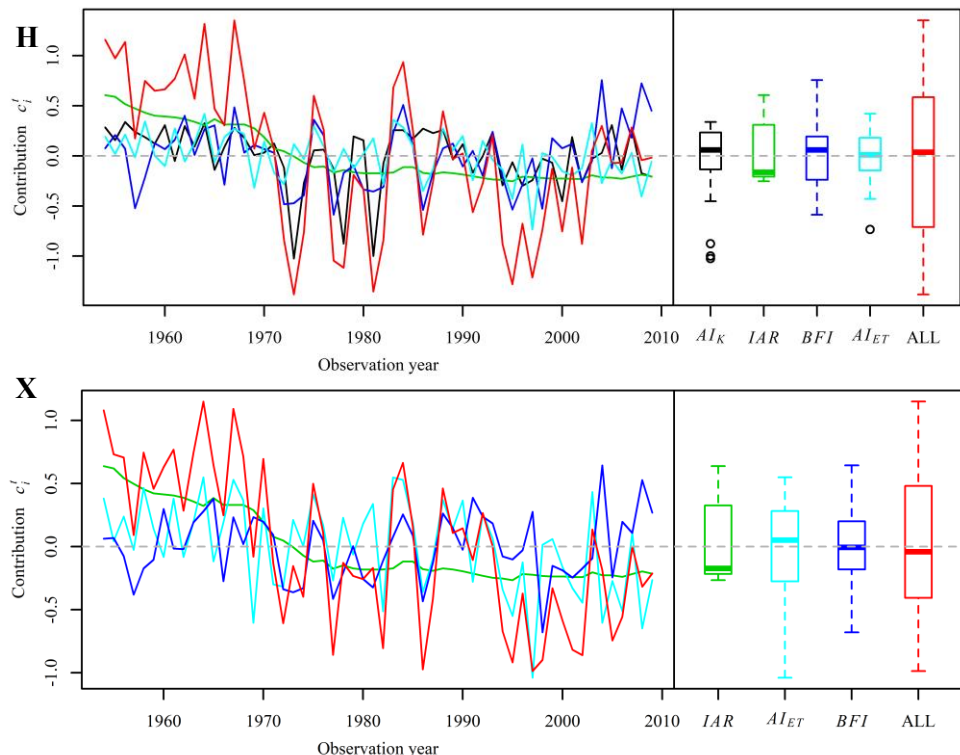
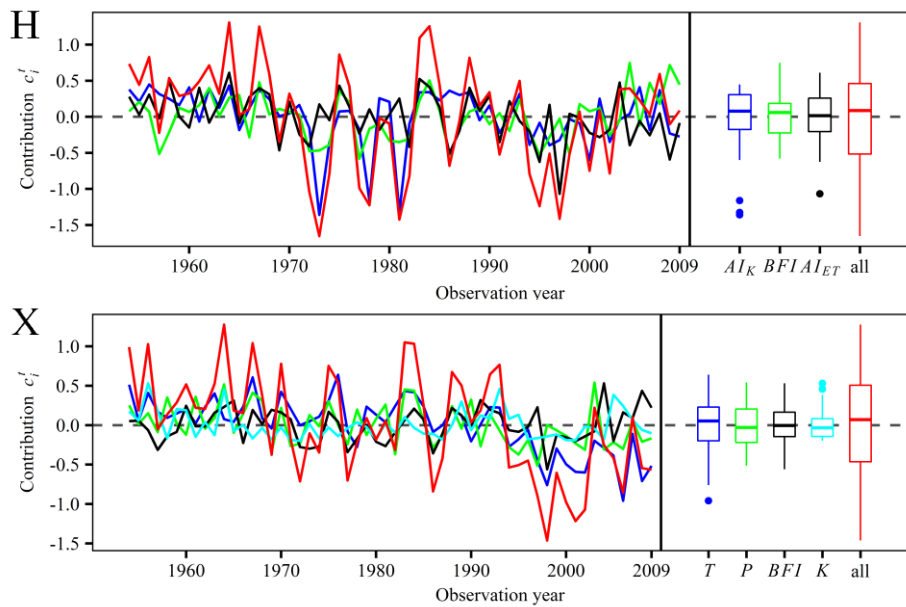
813 | Figure 89. Comparisons among of performance of stationary model (M0), time covariate model  
814 | (M1) and physical covariate models (M2a, M2b, M3, M4, M5 and M6 with the their  
815 | corresponding optimal explanatory variables) for AM<sub>30</sub> in Huaxian (H) at left panel and  
816 | Xianyang (X) at right panel.

817

818 | \_\_\_\_\_

**H****X**

823     Figure 910. Performance assessments of ~~the best M4 model (GA\_M4) GA\_M6~~ for  $AM_{30}$  in  
824     Huaxian (H) at left panel and Xianyang (X) at right panel. (a) and (b) are the centile curves plots  
825     of ~~GA\_M4 GA\_M6~~ (red lines represent the centile curves estimated by ~~GA\_M4 GA\_M6~~; the 50th  
826     centile curves are indicated by thick red; the yellow-filled areas are between the 5th and 95th  
827     centile curves; the filled black points indicate the observed series); (c) and (d) are the worm plots  
828     of ~~GA\_M4 GA\_M6~~ for the goodness-of-fit test; A reasonable model fit should have the data points  
829     fall within the 95% confidence intervals (between the two red dashed curves).  
830



833     | Figure 4011. Contribution of selected explanatory variables to  $c_i^t = \ln(\theta_i^t) - \ln(\bar{\theta}_i)$  in different  
834     | periods based on GA\_M4M6.

835

836

837

839 **Table**

840 Table 1. The probability density functions and moments (the mean and variance) for the candidate  
 841 distributions in this study.

Distributions	Probability density function	Distribution moments
Pearson-III	$f_Y(y \theta_1, \theta_2, \theta_3) = \frac{(y-\theta_3)^{\frac{1}{\theta_2^2}-1}}{\Gamma(1/\theta_2^2)(\theta_1\theta_2^2)^{\frac{1}{\theta_2^2}} \exp\left(-\frac{y-\theta_3}{\theta_1\theta_2^2}\right)}$ $y > \theta_3, \theta_3 > 0, \theta_1 > 0, \theta_2 > 0$	$E[Y] = \theta_1 + \theta_3$ $Var[Y] = \theta_1^2\theta_2^2$
Gamma	$f_Y(y \theta_1, \theta_2) = \frac{(y)^{\frac{1}{\theta_2^2}-1}}{\Gamma(1/\theta_2^2)(\theta_1\theta_2^2)^{\frac{1}{\theta_2^2}} \exp\left(-\frac{y}{\theta_1\theta_2^2}\right)}$ $y > 0, \theta_1 > 0, \theta_2 > 0$	$E[Y] = \theta_1$ $Var[Y] = \theta_1^2\theta_2^2$
Weibull	$f_Y(y \theta_1, \theta_2) = \left(\frac{\theta_2}{\theta_1}\right) \left(\frac{y}{\theta_1}\right)^{\frac{\theta_2-1}{\theta_2}} \exp\left(-\left(\frac{y}{\theta_1}\right)^{\frac{\theta_2}{\theta_2}}\right)$ $y > 0, \theta_1 > 0, \theta_2 > 0$	$E[Y] = \theta_1\Gamma(1+1/\theta_2)$ $Var[Y] = \theta_1^2 \left[ \Gamma\left(1+\frac{2}{\theta_2}\right) - \Gamma^2\left(1+\frac{1}{\theta_2}\right) \right]$
Lognormal	$f_Y(y \theta_1, \theta_2) = \frac{1}{y\theta_2\sqrt{2\pi}} \exp\left\{-\frac{[\log(y)-\theta_1]^2}{2\theta_2^2}\right\}$ $y > 0, \theta_2 > 0$	$E[Y] = w^{\theta_2} e^{\theta_1}$ $Var[Y] = w(w-1)e^{2\theta_1}$ $w = \exp(\theta_2^2)$
GEV	$f_Y(y \theta_1, \theta_2, \theta_3) = \frac{1}{\theta_2} \left[ 1 + \theta_3 \left( \frac{y-\theta_1}{\theta_2} \right) \right]^{-\frac{1}{\theta_2}-1} \exp\left\{-\left[ 1 + \theta_3 \left( \frac{y-\theta_1}{\theta_2} \right) \right]^{-\frac{1}{\theta_2}}\right\}$ $-\infty < \theta_1 < \infty, \theta_2 > 0, -\infty < \theta_3 < \infty$	$E[Y] = \theta_1 - \frac{\theta_2}{\theta_3} + \frac{\theta_2}{\theta_3} \eta_1$ $Var[Y] = \theta_2^2 (\eta_2 - \eta_1^2) / \theta_3^2$ $\eta_m = \Gamma(1-m\theta_3)$

843

Table 2. Description of the developed nonstationary models using time, or the indices of TCCCs  
 844 indices and/or HA indices as explanatory variables.

Model category	Codes	Distribution					Description	
		GA	WEI	LOGNO	PIII	GEV	Variable category	The numbers of variables
Nonstationary	M0	GA_M0	WEI_M0	LOGNO_M0	PIII_M0	GEV_M0	-	Zero
	M1	GA_M1	WEI_M1	LOGNO_M1	PIII_M1	GEV_M1	Time	One
	M2	GA_M2	WEI_M2	LOGNO_M2	PIII_M2	GEV_M2	TCCCs	One
	M3	GA_M3	WEI_M3	LOGNO_M3	PIII_M3	GEV_M3	TCCCs	Two
	M4	GA_M4	WEI_M4	LOGNO_M4	PIII_M4	GEV_M4	TCCCs	Identified by the stepwise selection

845

Model codes	Distribution					Description	
	GA	WEI	LOGNO	PIII	GEV	Variable category	The numbers of variables
M0	GA_M0	WEI_M0	LOGNO_M0	PIII_M0	GEV_M0	-	Zero
M1	GA_M1	WEI_M1	LOGNO_M1	PIII_M1	GEV_M1	Time	One
M2a	GA_M2a	WEI_M2a	LOGNO_M2a	PIII_M2a	GEV_M2a	TCCCs	One
M2b	GA_M2b	WEI_M2b	LOGNO_M2b	PIII_M2b	GEV_M2b	HA	One
M3	GA_M3	WEI_M3	LOGNO_M3	PIII_M3	GEV_M3	TCCCs	Two
M4	GA_M4	WEI_M4	LOGNO_M4	PIII_M4	GEV_M4	TCCCs	Identified by the stepwise selection
M5	GA_M5	WEI_M5	LOGNO_M5	PIII_M5	GEV_M5	HA	Identified by the stepwise selection
M6	GA_M6	WEI_M6	LOGNO_M6	PIII_M6	GEV_M6	TCCCs+HA	Identified by the stepwise selection

846

847

**Table 3. The summary of candidate explanatory variables and reason of selection.**

<u>Category</u>	<u>Name</u>	<u>Indices</u>	<u>Reason of selection (related to)</u>	<u>Unit</u>
<u>TCCCs</u>				
	<u>P</u>	<u>Precipitation</u>	<u>Main supply source</u>	<u>mm</u>
	<u><math>\lambda</math></u>	<u>Mean frequency of precipitation events</u>	<u>Water supply intensity</u>	<u>per day</u>
	<u>T</u>	<u>Temperature</u>	<u>Evaporation loss</u>	<u>°C</u>
	<u>ET</u>	<u>Potential evapotranspiration</u>	<u>Evaporation loss</u>	<u>mm</u>
	<u>AI<sub>ET</sub></u>	<u>Climate aridity index</u>	<u>Degree of meteorological drought</u>	<u>—</u>
	<u>BFI</u>	<u>Base-flow index</u>	<u>Water storage capability</u>	<u>—</u>
	<u>K</u>	<u>Recession constant</u>	<u>Water storage capability</u>	<u>day</u>
	<u>AI<sub>K</sub></u>	<u>Recession-related aridity index</u>	<u>Both the water storage and supply capability</u>	<u>—</u>
<u>HA</u>				
	<u>IAR</u>	<u>Irrigation area</u>	<u>Both irrigation diversion and evaporation loss</u>	<u>10<sup>6</sup> hm<sup>2</sup></u>
	<u>POP</u>	<u>Population</u>	<u>Water withdrawal loss for agricultural, domestic and industrial purposes</u>	<u>10<sup>6</sup></u>
	<u>GDP</u>	<u>Gross domestic product</u>	<u>Water withdrawal loss for agricultural, domestic and industrial purposes</u>	<u>10<sup>9</sup> ¥</u>

852 Table 34. The results of trend test and change-point detection for both the four low flow series and  
 853 eight candidate explanatory TCCCs variables in Huaxian and Xianyang stations.

Station	Variable	Mann-Kendall test		Pettitt's test	
		S	p-value	Change point	p-value
<b>Huaxian</b>					
	<i>AM</i> <sub>1</sub>	-564	6.91E-05(***)	1968	1.34E-03(**)
	<i>AM</i> <sub>7</sub>	-560	7.79E-05(***)	1968	1.44E-03(**)
	<i>AM</i> <sub>15</sub>	-438	2.01E-03(**)	1971	4.85E-03(**)
	<i>AM</i> <sub>30</sub>	-378	7.71E-03(**)	1971	9.96E-03(**)
	<i>P</i>	-292	3.97E-02(*)	1985	1.86E-01()
	$\lambda$	-632	8.20E-06(***)	1984	3.02E-04(***)
	<i>T</i>	752	1.11E-07(***)	1993	8.17E-06(***)
	<i>ET</i>	548	1.11E-04(***)	1993	1.98E-03(**)
	<i>AI</i> <sub>ET</sub>	384	6.79E-03(**)	1990	6.03E-02()
	<i>BFI</i>	52	7.19E-01()	1998	3.88E-01()
	<i>K</i>	-312	2.79E-02(*)	1968	8.11E-02()
	<i>AI</i> <sub>K</sub>	376	8.04E-03(**)	1971	3.60E-02(*)
<b>Xianyang</b>					
	<i>AM</i> <sub>1</sub>	-517	2.65E-04(***)	1968	2.2E-03(**)
	<i>AM</i> <sub>7</sub>	-483	6.58E-04(***)	1970	2.5E-03(**)
	<i>AM</i> <sub>15</sub>	-474	8.29E-04(***)	1971	2.2E-03(**)
	<i>AM</i> <sub>30</sub>	-570	5.78E-05(***)	1993	4.5E-04(***)
	<i>P</i>	-414	3.51E-03(**)	1990	1.45E-02(*)
	$\lambda$	-652	4.21E-06(***)	1984	6.00E-05(***)
	<i>T</i>	724	3.22E-07(***)	1993	5.41E-06(***)
	<i>ET</i>	372	8.74E-03(**)	1993	3.01E-03(**)
	<i>AI</i> <sub>ET</sub>	454	1.37E-03(**)	1993	8.82E-03(**)
	<i>BFI</i>	64	6.56E-01()	2003	8.65E-01()
	<i>K</i>	-210	1.39E-01()	1966	2.03E-01()
	<i>AI</i> <sub>K</sub>	290	4.11E-02(*)	1968	1.63E-01()

854 Signif. codes: 0 '\*\*\*' 0.001 '\*\*' 0.01 '\*' 0.05 '.' 0.1 ' ' 1

**Table 4. The results of M2 models for modeling low flow series in Huaxian and Xianyang stations.**

Station	Series	Optimal variable	Optimal distribution	AIC	Distribution parameters		
					$\ln(\theta_1)$	$\ln(\theta_2)$	$\theta_3$
Huaxian	$AM_+$	$AI_K$	WEI	95.0	$-0.19 - 0.72AI_K$	-0.418	-
	$AM_+$	$AI_K$	PHI	135.7	$-0.43 - 0.76AI_K$	0.219	0.007
	$AM_{45}$	$AI_K$	PHI	184.2	$0.83 - 0.75AI_K$	0.105	0.069
	$AM_{30}$	$AI_K$	GA	217.4	$-1.09 - 0.59AI_K$	-0.133	-
Xianyang	$AM_+$	$K$	GA	210.7	$1.00 + 0.40K$	-0.118	-
	$AM_+$	$AI_{ET}$	GA	228.4	$-1.17 - 0.45AI_{ET}$	-0.139	-
	$AM_{45}$	$AI_{ET}$	GA	251.0	$-1.39 - 0.49AI_{ET}$	-0.139	-
	$AM_{30}$	$T$	GA	270.1	$-1.59 - 0.50T$	-0.184	-

860 | Table 5. The summary of frequency analysis using GA distribution for  $AM_{30}$  in Huaxian and Xianyang.

Station	Model codes	Optimal variable	AIC	Distribution parameters		
				<u><math>\ln(\theta_1)</math></u>	<u><math>\ln(\theta_2)</math></u>	<u><math>\theta_3</math></u>
<u><b>Huaxian</b></u>						
	<u>GA_M0</u>	<u><math>z</math></u>	<u>232.3</u>	<u>1.09</u>	<u>-0.133</u>	<u><math>z</math></u>
	<u>GA_M1</u>	<u><math>t</math></u>	<u>225.5</u>	<u>1.09-0.32<math>t</math></u>	<u>-0.133</u>	<u><math>z</math></u>
	<u>GA_M2</u>	<u><math>AI_K</math></u>	<u>217.4</u>	<u>1.09-0.59<math>AI_K</math></u>	<u>-0.133</u>	<u><math>z</math></u>
	<u>GA_M2b</u>	<u><math>IAR</math></u>	<u>218.3</u>	<u>1.09-0.47<math>IAR</math></u>	<u>-0.133</u>	<u><math>z</math></u>
	<u>GA_M3</u>	<u><math>AI_K, BFI</math></u>	<u>213.7</u>	<u>1.09-0.50<math>AI_K</math>+0.32<math>BFI</math></u>	<u>-0.133</u>	<u><math>z</math></u>
	<u>GA_M4</u>	<u><math>AI_K, BFI, AI_{ET}</math></u>	<u>211.1</u>	<u>1.09-0.40<math>AI_K</math>+0.32<math>BFI</math>-0.34<math>AI_{ET}</math></u>	<u>-0.133</u>	<u><math>z</math></u>
	<u>GA_M5</u>	<u><math>IAR</math></u>	<u>218.3</u>	<u>1.09-0.47<math>IAR</math></u>	<u>-0.133</u>	<u><math>z</math></u>
	<u>GA_M6</u>	<u><math>AI_K, IAR, BFI, AI_{ET}</math></u>	<u>207.0</u>	<u>1.09-0.30<math>AI_K</math>-0.27<math>IAR</math>+0.32<math>BFI</math>-0.23<math>AI_{ET}</math></u>	<u>-0.133</u>	<u><math>z</math></u>
<u><b>Xianyang</b></u>						
	<u>GA_M0</u>	<u><math>z</math></u>	<u>285.8</u>	<u>1.59</u>	<u>-0.184</u>	<u><math>z</math></u>
	<u>GA_M1</u>	<u><math>t</math></u>	<u>270.1</u>	<u>1.59-0.48<math>t</math></u>	<u>-0.184</u>	<u><math>z</math></u>
	<u>GA_M2a</u>	<u><math>T</math></u>	<u>270.1</u>	<u>1.59-0.50<math>T</math></u>	<u>-0.184</u>	<u><math>z</math></u>
	<u>GA_M2b</u>	<u><math>IAR</math></u>	<u>267.8</u>	<u>1.59-0.50<math>IAR</math></u>	<u>-0.184</u>	<u><math>z</math></u>
	<u>GA_M3</u>	<u><math>T, P</math></u>	<u>267.1</u>	<u>1.59-0.34<math>T</math>+0.32<math>P</math></u>	<u>-0.184</u>	<u><math>z</math></u>
	<u>GA_M4</u>	<u><math>T, P, BFI, K</math></u>	<u>265.4</u>	<u>1.59-0.33<math>T</math>+0.27<math>P</math>+0.22<math>BFI</math>+0.18<math>K</math></u>	<u>-0.184</u>	<u><math>z</math></u>
	<u>GA_M5</u>	<u><math>IAR</math></u>	<u>267.8</u>	<u>1.59-0.50<math>IAR</math></u>	<u>-0.184</u>	<u><math>z</math></u>
	<u>GA_M6</u>	<u><math>IAR, AI_{ET}, BFI</math></u>	<u>259.7</u>	<u>1.59-0.28<math>IAR</math>-0.36<math>AI_{ET}</math>+0.26<math>BFI</math></u>	<u>-0.184+0.23<math>IAR</math></u>	<u><math>z</math></u>

861

862

**Table 5. The summary of frequency analysis for four annual low flow series of Huaxian.**

Series	Model codes	Optimal variable	AIC	Distribution parameters		
				$\ln(\theta_1)$	$\ln(\theta_2)$	$\theta_3$
<i>AM<sub>+</sub></i>	WEI_M0	-	104.6	-0.19	-0.418	-
	WEI_M1	<i>t</i>	91.1	-0.19-0.84 <i>t</i>	-0.418-0.30 <i>t</i>	-
	WEI_M2	<i>AI<sub>K</sub></i>	95.0	-0.19-0.72 <i>AI<sub>K</sub></i>	-0.418	-
	WEI_M3	<i>AI<sub>K</sub></i> , <i>BFI</i>	91.3	-0.19-0.58 <i>AI<sub>K</sub></i> -0.55 <i>BFI</i>	-0.418	-
	WEI_M4	<i>AI<sub>K</sub></i> , <i>BFI</i> , <i>ET</i> , $\lambda$	87.9	-0.19-0.39 <i>AI<sub>K</sub></i> +0.61 <i>BFI</i> -0.54 <i>ET</i>	-0.418-0.27 <i>t</i>	-
<i>AM<sub>-</sub></i>	PHH_M0	-	155.0	0.43	0.219	0.007
	PHH_M1	<i>t</i>	136.8	0.43-0.59 <i>t</i>	0.219+0.19 <i>t</i>	0.007
	PHH_M2	<i>AI<sub>K</sub></i>	135.7	0.43-0.76 <i>AI<sub>K</sub></i>	0.219	0.007
	PHH_M3	<i>AI<sub>K</sub></i> , <i>BFI</i>	132.4	0.43-0.65 <i>AI<sub>K</sub></i> -0.48 <i>BFI</i>	0.219	0.007
	PHH_M4	<i>AI<sub>K</sub></i> , <i>BFI</i> , <i>AI<sub>EF</sub></i> , $\lambda$ , <i>P</i>	127.5	0.43-0.62 <i>AI<sub>K</sub></i> -0.57 <i>BFI</i> -0.60 <i>AI<sub>EF</sub></i>	0.219-0.32-0.30 <i>AI<sub>K</sub></i> +0.21 <i>P</i>	0.007
<i>AM<sub>±</sub></i>	PHH_M0	-	203.5	0.83	0.105	0.069
	PHH_M1	<i>t</i>	188.0	0.83-0.46 <i>t</i>	0.105+0.208 <i>t</i>	0.069
	PHH_M2	<i>AI<sub>K</sub></i>	184.2	0.83-0.75 <i>AI<sub>K</sub></i>	0.105	0.069
	PHH_M3	<i>AI<sub>K</sub></i> , <i>BFI</i>	180.6	0.83-0.65 <i>AI<sub>K</sub></i> +0.43 <i>BFI</i>	0.105	0.069
	PHH_M4	<i>AI<sub>K</sub></i> , <i>BFI</i> , $\lambda$ , <i>K</i>	170.4	0.83-0.70 <i>AI<sub>K</sub></i> -0.42 <i>BFI</i>	0.105-0.36-0.71 <i>AI<sub>K</sub></i> -0.43 <i>K</i>	0.069
<i>AM<sub>30</sub></i>	GA_M0	-	232.3	1.09	-0.133	-
	GA_M1	<i>t</i>	225.5	1.09-0.32 <i>t</i>	-0.133	-
	GA_M2	<i>AI<sub>K</sub></i>	217.4	1.09-0.59 <i>AI<sub>K</sub></i>	-0.133	-
	GA_M3	<i>AI<sub>K</sub></i> , <i>BFI</i>	213.7	1.09-0.5 <i>AI<sub>K</sub></i> -0.32 <i>BFI</i>	-0.133	-
	GA_M4	<i>AI<sub>K</sub></i> , <i>BFI</i> , <i>AI<sub>T</sub></i>	211.1	1.09-0.4 <i>AI<sub>K</sub></i> +0.32 <i>BFI</i> -0.34 <i>AI<sub>T</sub></i>	-0.133	-

Table 6. The summary of frequency analysis for four annual low flow series of Xianyang.

Series	Model codes	Optimal variable	AIC	Distribution parameters	
				$\ln(\theta_1)$	$\ln(\theta_2)$
$AM_1$	GA_M0	-	222.3	1.0	-0.118
	GA_M1	$t$	209.9	1.0-0.44 $t$	-0.118
	GA_M2	$K$	210.7	1.0+0.4 $K$	-0.118
	GA_M3	$K, T$	204.3	1.0+0.37 $K$ -0.38 $T$	-0.118
	GA_M4	$K, T, BFI, \lambda$	203.2	1.0+0.33 $K$ -0.32 $T$ +0.27 $BFI$	-0.118-0.17 $\lambda$
$AM_2$	GA_M0	-	240.1	1.17	-0.139
	GA_M1	$t$	227.9	1.17-0.42 $t$	-0.139
	GA_M2	$AI_{EF}$	228.4	1.17-0.45 $AI_{EF}$	-0.139
	GA_M3	$AI_{EF}, K$	223.7	1.17-0.38 $AI_{EF}$ +0.31 $K$	-0.139
	GA_M4	$AI_{EF}, K, BFI, \lambda$	221.7	1.17-0.31 $AI_{EF}$ +0.3 $K$ +0.28 $BFI$	-0.139-0.21 $\lambda$
$AM_{15}$	GA_M0	-	265.3	1.39	-0.139
	GA_M1	$t$	253.4	1.39-0.43 $t$	-0.139
	GA_M2	$AI_{EF}$	251.0	1.39-0.49 $AI_{EF}$	-0.139
	GA_M3	$AI_{EF}, K$	249.2	1.39-0.45 $AI_{EF}$ +0.24 $K$	-0.139
	GA_M4	$AI_{EF}, K, BFI, \lambda$	246.6	1.39-0.36 $AI_{EF}$ +0.23 $K$ +0.32 $BFI$	-0.139-0.21 $\lambda$
$AM_{20}$	GA_M0	-	285.8	1.59	-0.184
	GA_M1	$t$	270.1	1.59-0.48 $t$	-0.184
	GA_M2	$T$	270.1	1.59-0.5 $T$	-0.184
	GA_M3	$T, P$	267.1	1.59-0.34 $T$ +0.32 $P$	-0.184
	GA_M4	$T, P, BFI, K$	265.4	1.59-0.33 $T$ +0.27 $P$ +0.22 $BFI$ +0.18 $K$	-0.184